Particle Accelerators
1979, Vol. 10, pp. 1-30
0031-2460/79/1001-0001$04.50/0

HIGH-POWER ELECTRON AND ION BEAM GENERATION

JOHN A. NATION

Laboratory of Plasma Studies
and
School of Electrical Engineering
Cornell University, Ithaca, New York 14853

(Received January 29, 1979)

In this review we present an introduction to and summary of high-power electron and ion-beam technology. The research areas covered are diverse and have not all been previously summarized in a review. An effort has been made to include unpublished data on dielectric strengths and breakdown times in sufficient detail to be useful. Descriptions are presented of the essential machine components and their limitations from the design viewpoint. The physics of the electron and ion beam generating diodes are given, together with a summary of achieved beam characteristics. The review concludes with a brief summary of progress in the study of the collective ion acceleration, which may occur in high-current electron beams.

I. INTRODUCTION

There has been a rapid development since the early 1960's of new pulsed-power sources. These sources range from small 500-kV, 70-kA generators to large multi-terawatt sources such as the Aurora generator at the Harry Diamond Laboratories (14 MV, 1.6 MA). These generators, which were developed as devices for materials testing and as x-ray sources, typically produce high-power pulses for times of about 50–100 nsec. The generators, which can be operated in either polarity, have recently been utilized for a variety of other applications including controlled thermonuclear fusion,[1-6] and microwave generation.[7-8] In this review we shall describe the general characteristics of these beam devices, including the production of high-energy ion beams by collective processes,[9-11] but will not discuss applications other than to indicate the requirements they set on machine characteristics.

In the following sections we shall discuss the basic machine technology and illustrate this with reference to specific devices. The machines which have been constructed consist of three or more essential elements, an energy-storage device such as a Marx generator, a pulse-forming network, and a diode used for beam generation. The pulse line provides a fast-rise, short-duration pulse which is applied to the vacuum diode. The detailed design of the diode depends on whether the generator is to be operated in positive or negative polarity. For use as an ion-beam source it is necessary to suppress the electron flow, or at least to make the resistance to electron flow across the diode comparable to that for protons. We shall discuss the different configurations used for electron and ion beam generation and their relative efficiencies. In recent experiments ion beams have been generated at power levels approaching a terawatt.

Most of the work carried out to date has been aimed at producing ultra-high power electron beams at low impedance levels ($\lesssim 1$ ohm). Although multi-terrawatt generators such as the Aurora machine (see Table I) have also been built, relatively little effort has been devoted to the production of modular, moderate-impedance, high-power, high-voltage pulses. A specific method of pulsed-power technology which has addressed this problem is the induction linac. In this device conventional pulsed-power systems are used to feed an inductive load. A particle beam in parallel with the ferrite load is accelerated by a changing magnetic field. Although little development has occurred in these systems in the last several years, the principle has been tested with the successful acceleration of several hundred amperes of electrons through a multi-stage system. This type of accelerator is currently being assessed as a 10-kA source of high-energy (50-MeV) electrons, and as an accelerator for use in heavy-ion fusion applications.

Since this review is concerned with the current research in high-power electron and ion accelerators, it is also appropriate to examine the present status of collective-ion acceleration in intense relativistic electron beams. There has been some resurgence of interest in this field in the last few years, as electron-beam technology has advanced, and

several groups are actively engaged in investigations of collective-acceleration processes. At present, most of the research has been concerned with the ion acceleration which can occur as the head of an electron beam propagates into a neutral gas, or into vacuum through a dielectric window. The most encouraging results show that proton energies of up to about 22 times the electron-beam energy have been achieved. There are also more recent efforts at controlled collective acceleration using either a wave train for the trapping and subsequent acceleration of the ions or an accelerating solitary wave. The present status of this work will also be examined.

II. MACHINE TECHNOLOGY

A. Introduction

High pulsed-power systems development was initiated at the Atomic Weapons Research Establishment in England in 1962. At that time, J. C. Martin successfully combined existing Marx-generator technology, which could be used to generate megavolt pulses with rise times of the order of microseconds, with transmission-line systems to produce short ($\simeq$ 50 nsec) duration, high-power pulses. This process required the solution to a number of technological problems ranging from interfacing compact Marx generators with pulse-forming lines to fast-switch development and finally to the coupling of sub-microsecond pulses from the pulse lines to vacuum diodes for the generation of high-power electron beams. Since that time, the development of this technology has proceeded rapidly to the point where multi-terawatt electron-beam generators are now available. The final system depends considerably on the application of the high-power pulse. Pellet fusion systems using electron or proton beams require pulse powers approaching 10^{14} watts at beam energies in the range of one to ten mega-electron volts.[12] In contrast to this, heavy-ion fusion systems require a beam energy of about 10–100 GeV in a 100-terawatt system.[13] Other applications, such as the generation of electron and ion rings for magnetic confinement of a fusion plasma,[14] show that higher energy beams will be needed than are required for electron-pellet fusion. Similarly flash x-ray sources may require, for maximum x-ray yield, higher-voltage operation to capitalize on the fact that the x-ray yield depends on the cube of the beam energy. For application to microwave generation, high-impedance machines are required, since these devices typically operate in vacuum where the electron-beam current is limited by space-charge considerations.[15–17] In summary, we find that the various applications of pulsed-power technology lead to beam requirements ranging from sub-ohm impedance, multi-terawatt systems to relatively modest megavolt generators having impedances of several hundred ohms. Table I lists the characteristics of several multi-terawatt generators. The basic technology of each of these generators is essentially identical. The development from the work of J. C. Martin and his group has occurred in a number of laboratories throughout the world and includes major programs in the U.S.A. and the U.S.S.R. In this paper we shall utilize developments in the U.S.A. to characterize machine systems. The study and development of the pulsed-power systems in the U.S.A. has occurred at several laboratories, including Cornell University, Ion Physics Co., Maxwell Laboratories, Naval Research Laboratories, Physics International Co., and Sandia Laboratories.

Figure 1† shows a block diagram illustrating the principal components of a pulse generator. A Marx generator is used to impulse charge a pulse-forming line to high voltage. Charging is usually accomplished in less than a microsecond, so that the Marx must have a low inductance. The pulsed line is usually a Blumlein transmission line; it employs a water dielectric for low-impedance, moderate-voltage applications, or oil for high voltage use. The Blumlein has the advantage over a simple coaxial pulse line that it is capable of delivering the full charging voltage to a matched load. As shown in the figure, a transmission line couples the vacuum diode to the Blumlein. In some applications, the coupling line may also serve as a transformer to increase or decrease the characteristic impedance of the pulse. The vacuum diode is coupled to the electron-beam generation region through a solid-dielectric interface which may consist of a stacked, graded axial-ring assembly or a lower-inductance radial insulator. In pellet-fusion applications, an additional section is needed to provide the high ($\gtrsim 10^{11}$ W/cm^2) power densities required. This is provided by several long runs of magnetically insulated transmission line. We now discuss each of these components in more detail.

† Pulsed-power systems using Van de Graaff generators are also in use. They are less common, however, than the Marx Generator, pulse-line systems, and also less flexible. They do provide extremely stable sources with excellent repetition characteristics. They will not be discussed in this review.

TABLE I
Output characteristics of some multi-terawatt generators

Machine name	Voltage (MV)	Current (MA)	Pulse duration (nsec)	Power (TW)
Aurora	14	1.6	120	22
Hermes II	10	0.1	80	1
Proto II	1.5	6.0	24	9
Gamble II	1.0	1.0	50	1
Blackjack	1.3	1.1	50	1.4
Owl	1.5	0.75	110	1.2

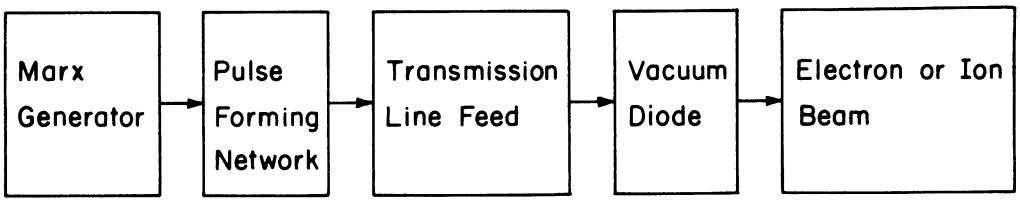

FIGURE 1 Block diagram of a typical high power pulse generator.

B. Marx Generators

A simplified schematic of a section of a Marx generator is given in Fig. 2. In the configuration shown, we have illustrated an $n = 2$ Marx. This arrangement is capable of erection, following the triggering of at least the first gap, at voltages approaching half the self-breakdown voltage of each individual gap. This configuration has been successfully used for the construction of a number of Marx generators with energies in the range of 100 kJ.

The system consists of a series of capacitors C_0 charged in parallel through the charging lines and ground returns. The system has stray capacitance C_g across each spark gap and is arranged so that there is a large C_c (compared to C_g) capacitance across every two spark gaps. To illustrate the rationale for the design, we consider the situation prevailing at the point A in the column. We assume that the previous $(p\text{-}1)$ spark gaps have closed so that the potential at the point A *is* pV_0, where V_0 is the charging voltage of each of the Marx capacitors. After erection of the column to the point A, the gap capacitor C_g and the coupling capacitor C_c act a voltage divider and the potential at the point B is

$$V_B = (p=2)\,V_0 + 2V_0 \frac{C_g}{C_g + C_c} . \qquad (1)$$

Hence the potential difference across the gap V_{BA} is

$$V_{BA} = \frac{2V_0\, C_c}{(C_c + C_g)} . \qquad (2)$$

The coupling capacitor discharges through the charging resistor in a time of order RC_c and leaves the potential difference across the gap at twice the capacitor charging voltage, i.e., $V_{BA} = 2V_0$. The fact that the gap potential difference tends to $2V_0$ is characteristic of the $n = 2$ Marx configuration, in which the coupling capacitors C_c are made large across every two spark gaps, and because the charging and ground-return resistors also straddle two gaps. In an $n = 3$ configuration, the charging resistors couple three spark gaps and coupling capacitors C_c are made large across every third gap. For an $n = 3$ Marx, the gap voltage approaches $3V_0$ when the preceding two gaps have been triggered, and the Marx can erect, after triggering of the early gaps, with voltages of down to about one third of the self-break voltage of the individual gaps.

The high-n Marx configurations are relatively free from self-breakdown problems, but tend to erect more slowly than less complex configurations. It is not always best to use self-erecting Marx generators and in some cases it is preferable to trigger all the spark gaps. In such cases, trigger gaps may be coupled using a similar configuration in the trigger

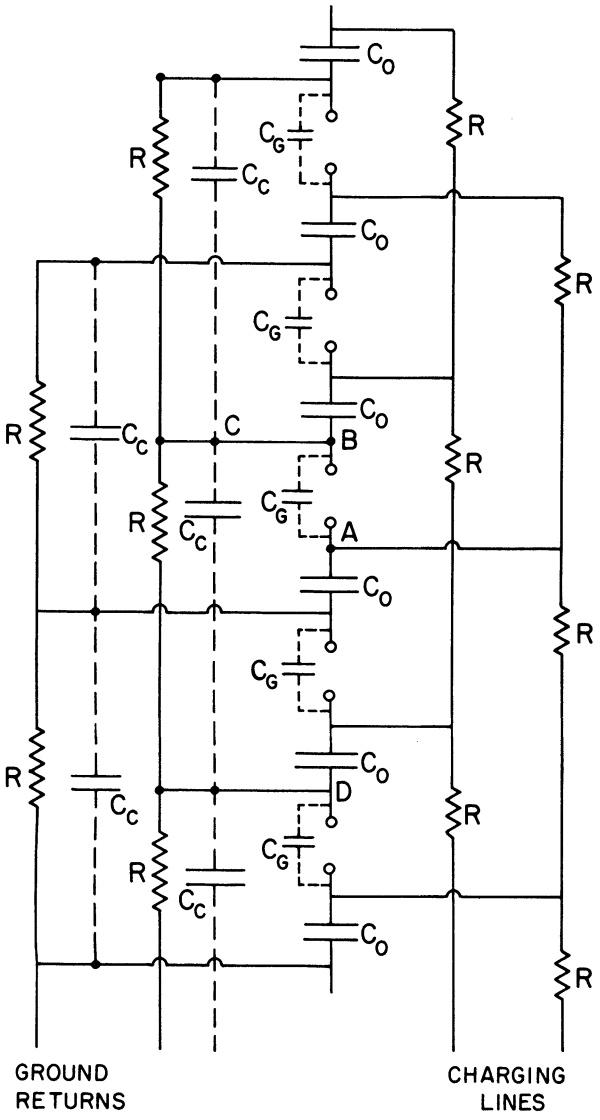

FIGURE 2 Simplified schematic of self triggered $n = 2$ Marx generator.

leads to that used for the charging columns and coupling capacitors in the self-erecting Marx. The use of plus-minus charging of alternate capacitors also enables one to reduce the number of switches required by a factor of two.

In most generators built, the charging and trigger resistors are made from copper-sulfate solution in flexible plastic tubing. These resistors are capable of high power dissipation and are also flexible enough that they can be contoured to suit the electrical stressing requirements of the generator.

In some large electron-beam generators designed to operate at low impedance, multiple Marx generators have been used as storage elements. For example, in the Proto II[18] generator at Sandia Laboratories, eight 112-kJ Marx generators are used in parallel to charge the fast line sections. This provides a lower-inductance and a faster rise-time system than could be achieved with a single large generator. Each Marx generator in this case consists of 32 0.7-μF, 100-kV capacitors. The equivalent circuit of the erected Marx generator has an output capacitance of 22 nF in series with an inductance of about 7 μH. The Marx has a series resistance of about 3 ohms and is shunted by 560 ohms.

One of the largest generators built to date, the Aurora facility,[19] has four Marx generators, each of which contains a 95 stage Marx generator with each stage consisting of four 1.85-μF, 60-kV capacitors wired as a 1.85-μF, 120-kV unit. The total energy storage in the generator is 5 MJ. The generator is a so-called hybrid Marx in which the coupling stray capacitors, and resistively coupled triggers are the dominant components in determining the column erection. The illustration of Fig. 2 shows an RC-coupled, self-erecting Marx.

A very low inductance variation of the Marx generator has been developed by Fitch and Howell.[20] This is called an LC Marx Generator and is shown in Fig. 3. In this configuration, alternate capacitors are charged with opposite polarities. On closing the switches, the column erects, reaching peak voltage in the half period of the resonant circuits. This circuit may be constructed with a low inductance, but is also prone to several different fault modes of operation, where, for example, not all of the gaps close at the proper time. Such faults may result in over-stressing, or ringing, of individual elements.

We conclude our discussion of Marx generators by noting that in certain applications the Marx generator has been directly coupled to a vacuum diode and has been used to produce a long-duration particle beam.[21,22] Beam durations of a few microseconds have been achieved and have been used for microwave generation and for electron and ion-beam production for plasma heating and containment systems. In this mode of operation, the beam rise time is much slower than that found with pulse lines and the generator impedance is relatively high, typically of the order of several tens of ohms. The shape of the pulse depends on the application but, if required, can be controlled using one or more stages of output filtering to give a 'square' pulse while

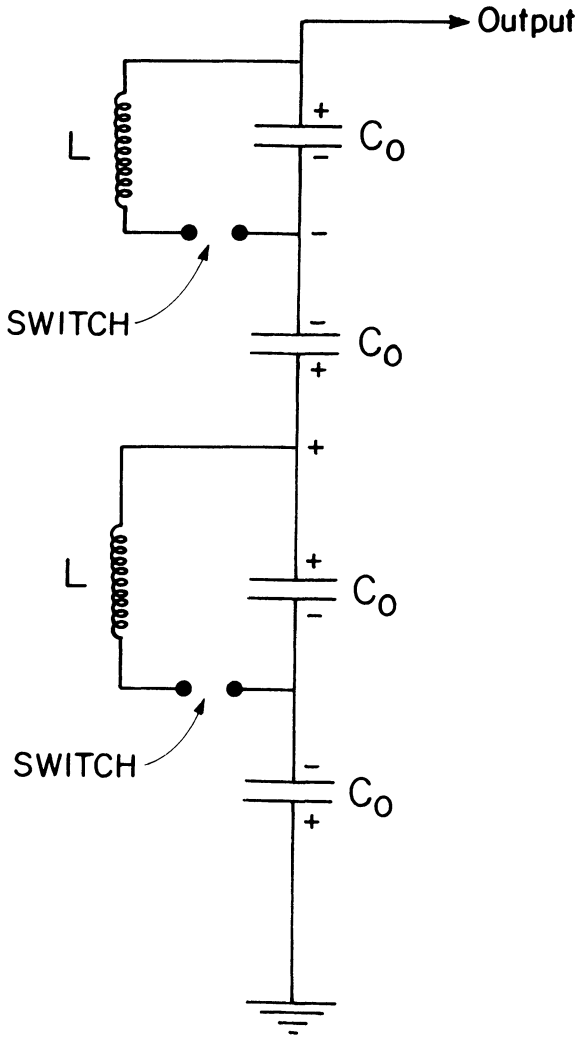

FIGURE 3 Simplified schematic of a four stage LC Marx generator. The capacitors are charged as shown. For simplicity the charging and triggering currents have been omitted.

maintaining an efficient transfer of energy from the primary Marx store to the beam.

C. Pulse-Forming Network

Marx generators are primary energy stores which can be used to energize a fast pulse-forming section in a time of order one microsecond. The fast section or pulse-forming network essentially consists of a transmission line that is charged from the Marx generator as a lumped capacitor, and is discharged in the transmission-line mode. The output pulse is fed to a vacuum diode which is used to generate the particle beam. The fast section typically produces an order of magnitude decrease in the pulse duration and a corresponding increase in the power output. Figure 4 shows schematically a Blumlein transmission-line system. This circuit, which was devised by A. D. Blumlein,[23] enables one to produce an output pulse into a matched load equal to the original charging voltage of the line. This is, of course, in contrast to the simple pulse line which delivers half of the charging voltage across a matched load.

In many instances, the Blumlein circuit consists of three coaxial cylinders with the intermediate cylinder charged from the Marx generator. There are also a number of refinements of this basic circuit which may be used to enhance the triggering capability or to modify the output characteristics. We shall discuss the basic principles first and subsequently outline specific modifications necessary for the special applications.

The intermediate conductor of the coaxial Blumlein is charged from the Marx generator in a time of the order of or less than one microsecond. Typical dielectrics used to insulate the conductors are deionized water or transformer oil. The RC discharge time for 10^4 Ωm water in cylindrical geometry is $\rho\varepsilon \sim 7$ μsec. Hence, submicrosecond charging times are adequate. The insulating interfaces are commonly made of lucite or some other plastic. These interfaces may also serve as supports for the conductors. The center conductor of the Blumlein is electrically connected to the outer grounded cylinder by a few microhenry inductor. The inductor ideally acts as a short circuit during the 1-μsec charging of the line and as an open circuit, compared to the characteristic impedance of the line, on the output-pulse duration time scale. The output impedance of the generator is equal to the sum of the characteristic impedances of the separate coaxial sections. The matched load impedance is therefore equal to the characteristic impedance of the section of coaxial line separating the Blumlein section from the load. This latter section is also helpful in reducing the prepulse voltage, which appears across the diode gap during the charging cycle, due to the unequal charging rates of the two halves of the Blumlein. The prepulse may be further reduced by the addition of a gas prepulse-suppression switch prior to the diode. Provided that the switch has a low capacitance compared to the diode assembly plus the feed section on the diode side of the switch, the switch will capacitively divide any prepulse voltage according to the capacitance distribution. As shown in the figure, the line is switched at one end and left

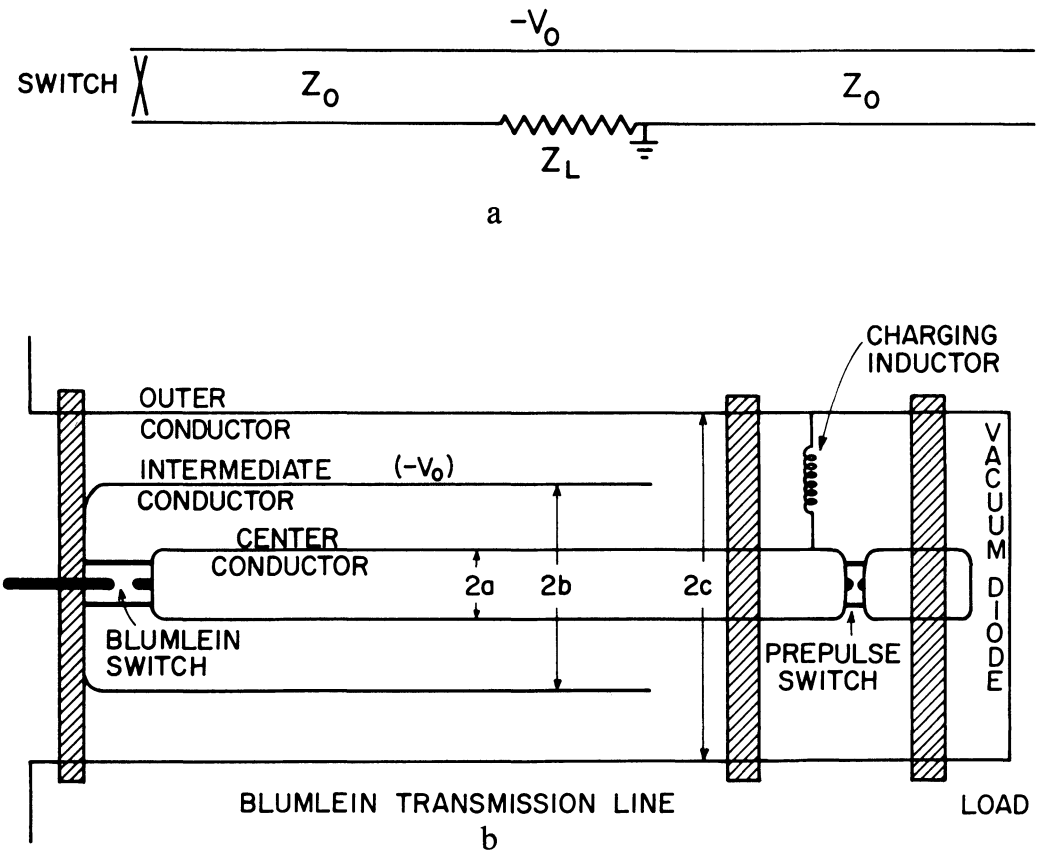

FIGURE 4 a) Blumlein transmission line. The line is charged to voltage V_0 on either side of the load, which in a matched configuration will have an impedance of $2Z_0$, twice the characteristic impedance of either section of the line. b) Cylindrical Blumlein transmission line.

open-circuit at the other. The load is located in the center (Fig. 4a) of the pulse-line system. The switch may be either a self-breaking liquid or gas switch or a triggered switch.

Almost all Blumlein configurations constructed to date have the geometry shown in Fig. 4b. In some cases, however, epecially where there is a need to synchronize the firing of many separate Blumleins, it may be useful to use the configuration sketched in Fig. 5, in which the switch is readily accessible. The high-voltage connection to the intermediate conductor is, however, less accessible. This latter configuration has been used in the Berkeley electron-ring accelerator pulse lines. It is electrically equivalent to the configuration illustrated in Fig. 4. Accounts describing the design and characteristics of several generators may be found in Refs. 24-34.

We now discuss some of the properties of different dielectrics and of different switching systems used in high-power pulse lines. Most of this data is based on the unpublished work of J. C. Martin[35] of Aldermaston.

D. Breakdown Characteristics of Insulators

We consider in this section the insulation properties of the common dielectrics used in pulse-forming networks. In cylindrical lines of the form previously described, the most commonly used dielectrics are water and transformer oil. Due to its high dielectric constant ($\varepsilon_r = 81$ at frequencies up to about 3 GHz), water provides a useful high energy-density storage medium, capable of storing energy at a density of about 160 kJ/m^3. In addition, the velocity of propagation of an electromagnetic wave through the water is c/9, so that water pulse-forming lines may be quite compact ($\sim$ 1 m long for a 50-nsec pulse). In contrast, the dielectric constant of oil is about 2.4, so

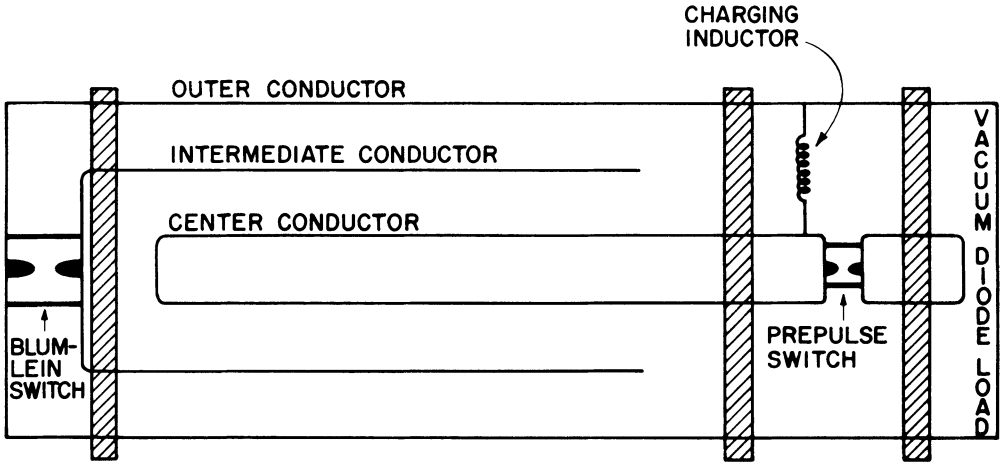

FIGURE 5 Cylindrical Blumlein with switching reversed.

that a 50-nsec Blumlein system would have a length of approximately 5.5 m. Oil may be used to store energy at a density of about 18 kJ/m^3.

J. C. Martin has shown that the dielectric strength of these liquids in uniform fields obeys a relation of the form

$$E_{BD}t^{1/3}A^{1/10} = k, \tag{3}$$

where E_{BD} is the breakdown electric-field strength of the liquid, A the electrode area and t the effective (submicrosecond) time duration of the high voltage. To compensate for rise time effects, in determining t we use only the time that the applied electric field exceeds 63% of its breakdown value. The constant k is polarity-dependent (denoted by the subscripts + and −). In mks units, k has the values given in Table II. Note that in water the breakdown is mainly determined by the positive-polarity electrode. For microsecond charging pulses, the breakdown strengths are about 15 MV/m for water and 25 MV/m for oil, where an electrode area of 0.1 m^2 has been assumed.

For short-duration (7–30 nsec), sub-megavolt pulses, VanDevender and Martin[36] have shown that the electric field at breakdown may be almost twice as large as predicted by Eq. (3). This result is important for electron-beam pellet-fusion systems, where the breakdown strength determines the current-handling capability of a vacuum diode [(Eq. (14)]. The breakdown field for these short-duration pulses is given by

$$E_{BD} = \frac{1.6 \times 10^6 d^{0.65}}{t^{0.39} A^{0.06}} . \tag{4}$$

In this case, as will be presented later for asymmetric electrode breakdown, it is not possible to describe the breakdown process without including an electrode separation factor d.

For the coaxial Blumlein configurations shown in Figs. 4 and 5, the electric field most likely to lead to breakdown is at the surface of the center conductor and has a value given by

$$E(a) = \frac{V\sqrt{\varepsilon_r Z_{ba}}}{60\,a} , \tag{5}$$

where V is the charging voltage, ε_r the relative permittivity of the dielectric and Z_{ba} the characteristic impedance of the coaxial section between the intermediate and center conductors. The breakdown criterion in water for electron-beam operation, i.e., in the negative-charge mode, is relatively worse than the positive-charge mode due to the polarity dif-

TABLE II

Values of constants k_+ and k_- used in determining the breakdown strength of water and oil

	k_+	k_-
Oil	2.0×10^5	2.0×10^5
Water	1.2×10^5	2.4×10^5

ference between the constants k. Following the closure of the switch, the center conductor becomes negative and is usually the most strongly stressed electrode. Due, however, to the short pulse duration compared with the charging time, the permitted electric field at the high-voltage conductor is much greater than that allowed during the charging phase.

In positive-polarity operation (i.e., for the generation of proton beams), the intermediate conductor has the greatest stress during the charging cycle, although the stressing obtained is weaker, due to the larger radius of the intermediate conductor. If a machine is required for use in both the electron and ion beam modes, then it may be a useful compromise to work with a system in which $Z_{CB}/Z_{BA} = b/a$.

In a coaxial system, the electric-field variation, at fixed potential difference between the conductors, has the form

$$E(r) = \frac{V}{r \ln\left(\frac{c}{r}\right)}, \tag{6}$$

where the outer conductor radius has been taken as c meters. It is straightforward to show that the electric field at radius r is a minimum when the logarithmic factor is unity. This result leads naturally to a preferred impedance range for a given dielectric. Water lines operate typically around 7 ohms, whereas oil is characteristically used in higher voltage applications at impedances of about 35 ohms.

A number of pulse-forming networks have utilized strip transmission lines for the fast section of the beam generator. In such a device, it is often possible to use a solid dielectric insulator such as Mylar. For uniform-field configurations, the breakdown field strength is volume-dependent, but essentially time-independent:

$$E_{BD}\,(V)^{1/10} = k, \tag{7}$$

where the constant k has a value of about 7.5×10^7 in mks units. The volume (V) dependence in the above relation and the area dependence in Eq. (3) for the breakdown of liquids are very similar. In the solid case, the volume is relevant since breakdown may originate anywhere in the insulating volume. In contrast, breakdown usually commences on the surface of a liquid. The exponents in both cases reflect the fact that the breakdown strength of a sample (liquid or solid) has intrinsic scatter corresponding to a standard deviation of about 10%. The mean value of the breakdown field strength is then sample-size dependent† and for the quoted standard deviation corresponds to a 1/10th power of the sample size. In gases, the intrinsic spread in the breakdown strength is an order of magnitude less and there is no significant volume effect, except in the largest of the Van de Graaff machines. The solid-dielectric systems employing plastic insulating sheets may be stressed to fields approaching 300 MV/m and are capable of storing energy at densities of greater than 1 MJ/m^3. We note in passing that the electric-field strength close to the edge of a strip-line conductor may be substantially greater than the average value between the plates. The stressing is usually relieved and the air voids between the dielectric sheets filled by immersing the whole line in a weakly conducting copper-sulfate solution. The solution serves as part of an RC network giving an effective radius of a few mm to the otherwise-sharp conductor boundaries.

The switching of a charged Blumlein into a load requires the reliable firing of a normally insulating gap. That is, we are interested in obtaining a failure of the insulation properties of the dielectric at a prescribed location, and at a predetermined time or voltage. This has been achieved by either using the self-breakdown of gaps or by deliberate triggering of the system. We deal in this review with the self-triggering situation. The breakdown of a switch follows similar laws to those given earlier for the breakdown of dielectric in a uniform field. In this case, however, breakdown is desired at a predetermined level and location. This is achieved by using nonuniform field configurations where the breakdown is required. Consider, for example, the self-breakdown of a Blumlein switch constructed of the same dielectric as is used to insulate the line. Table III gives phenomenological relations describing the breakdown characteristics for an edge-plane gap. As in the uniform field, there is a polarity effect, which for water continues to exhibit the preferential breakdown from the positive edge. At submegavolt voltages the oil breakdown is dominated by the negative edge. The breakdown fields given correspond to the average electric field across the gap and are typically in the range of about half the breakdown field strengths for the uniform gap

† The breakdown probability of a dielectric follows a Weibull distribution. Volume or area effects in determining dielectric strengths may be inferred from a knowledge of the breakdown statistics of a single (fixed volume or area) sample. For example, *N successive stressings of a volume V* is equivalent to a single stressing of a volume N_V.

TABLE III

Relationships describing the average electric field causing breakdown between an edge and a plane in water and oil. d is the gap between the electrodes and t is the time the field exceeds 63% of the breakdown field.

	Negative edge	Positive edge
Water ($0.1 < V < 1.0$ MV)	$E_{BD}t^{0.61}d^{0.09} = 1160$	$E_{BD}t^{0.83}d^{-0.67} = 610$
Water ($1.0 < V < 3.0$ MV)	$E_{BD}t^{0.5} = 1.3 \times 10^4$	$E_{BD}t^{0.4} = 4.38 \times 10^4$
Oil ($0.1 < V < 1.0$ MV)	$E_{BD}t^{0.78}d^{0.22} = 50$	$E_{BD}t^{0.57}d^{0.43} = 400$
Oil ($1.0 < V < 5.0$ MV)	$E_{BD}t^{0.63}d^{0.22} = 392$	$E_{BD}t^{0.63}d^{0.22} = 392$

stressing. The relatively rapid variation of the breakdown strength with time for the water case has been utilized in the development of fast low-jitter switches for the triggering of low-impedance, short-duration pulses. For short-duration charging times and rapidly rising pulses, standard deviations in gap triggering of 2 to 3% have been obtained. An important additional benefit is that the gaps break down simultaneously in multiple channels, leading to very low-inductance switches. The multiple breakdown can only occur when the channels are transit-time isolated.

The self-breaking of water switches has, for example, been used in the development of the multiple-source generator, Proto II. To achieve the multiple firing with sufficiently low jitter, the Marx generators are used to charge water-dielectric storage capacitors. These capacitors are switched, via triggered SF_6 gaps, into a water transmission line in about 300 nsec. The lines self-break, in over 100 channels each, transferring their energy into the feeds to the load. The intermediate capacitor and the water line both act to speed up the energy transfer time and hence permit consistent low-jitter firing of the final gaps. The charging time of the lines using this sequencing is a factor of three faster than could be achieved using the Marx generators alone, and the jitter in the firing an order of magnitude lower than could be obtained otherwise. The water transfer capacitor system has also been used in a number of other pulse-line facilities to enhance trigger reproducibility and also to reduce the trigger inductance. The latter effect arises due to the closure of multiple switching channels in the rapid-charging configuration.

Gas switching is in common use in a number of pulse-line systems, especially in cases where the line impedance is moderately high (several ohms or greater). Four gases are in common use in switch applications (or for insulation in low-voltage Marx generators). They are air, nitrogen, freon, or sulfur hexafluoride. In uniform fields, the breakdown of air or nitrogen has been shown to satisfy the relation

$$E_B = \frac{1}{F}\left[24.6p + 210\left(\frac{p}{d_{\text{eff}}}\right)^{1/2}\right], \tag{8}$$

where p is the pressure, and all quantities are given in mks units. The breakdown of sulfur hexafluoride or freon occurs at fields approximately two and a half and five times greater than that given above. Note that freon is not the preferred gas in switches because carbon is formed during discharges in freon. In the above relationship, the distance d_{eff} defines an effective gap separation for the electrodes and F represents a field enhancement factor for the switch geometry. In planar geometry d_{eff} equals the actual electrode separation and F is unity. Values of F have been given by Alston for cylindrical and spherical electrodes. Table IV defines d_{eff} and F for a gap with a spacing equal to the electrode diameter (d). Values of d_{eff}/d and F are given for other aspect ratios by Alston.[37]

Since avalanche breakdown and streamer formation in gaps take a finite time to develop, it is possible to apply greater stress across gaps for ultrashort pulse durations (< 10 nsec). The time dependence for the breakdown of asymmetric gaps, such as point-plane, has a polarity effect which may be adequately described by a relation of the form

$$E_{BD} = \frac{k_{\pm}\, p^n}{(dt)^{1/6}}, \tag{9}$$

TABLE IV

Effective gap length and field enhancement factors for typical switch geometries

Electrode shape	d_{eff}/d	F
Cylinders	0.115	1.3
Spheres	0.057	1.8

TABLE V
Values of the constants used in Eq. (9) for the determination of the time dependence of the breakdown of gas switches

	Air	Freon	Sulfur Hexafluoride
k_+	1.02	16.7	20.4
k_-	1.02	27.8	33.4
n	0.6	0.4	0.4

where the constants k and n have the values given in Table V. In a similar manner to the previous case for the breakdown of a solid or liquid, the time factor allows for the relatively unimportant low-voltage part of the applied voltage pulse by taking t as the time the voltage exceeds 89% of the breakdown voltage. E_{BD} is the average field across the gap. The relations for gas breakdown are limited to pressures of less than about five atmospheres, although in the case of sulfur hexafluoride they apply up to about ten atmospheres; the relations were also obtained with gap lengths greater than about 10 cm.

The performance of a switch is determined not only by its breakdown characteristics but also by its rise time. This is controlled by two factors, the switch inductance and the drop in resistance of the channel due to its expansion associated with ohmic plasma heating. The relative importance of these terms depends on the detailed switch conditions. The time for the inductive-current rise in a circuit or the voltage fall across a switch having an inductance L and being driven by a circuit having an impedance Z is

$$\tau_L = \frac{L}{Z} . \tag{10}$$

The corresponding term for the resistive phase has been shown to be

$$\tau_R = \frac{7.8\ \rho^{1/2}}{Z^{1/3}\ E^{4/3}} , \tag{11}$$

Note that these are e-folding times for the switch and that the actual 10–90% rise time is not simply related to the above times when the individual time constants τ_R and τ_L are comparable.

In low-impedance machines, where the rise-time effects may limit the useful pulse duration,† it is sometimes more useful to switch the pulse-forming network at higher impedance, and then transform the impedance to the lower value required using a tapered transmission line. Figure 6 shows schematically a pulse-line transformer. If Z_0 and Z_i represent the output and input impedances of the tapered section, then the output characteristics are related to the input parameters by the relations

$$\frac{V_0}{V_i} = \frac{I_i}{I_0} = \left(\frac{Z_0}{Z_i}\right)^{1/2} . \tag{13}$$

These relations assume that the change in line impedance is adiabatic, and that the tapered section has a length comparable to or greater than the length of the pulse. A step-down transformer has been used in the Naval Research Laboratory (NRL) generator Gamble II[29] to minimize the pulse rise time. Step-up transformers have been used, for example, on the VEBA facility at NRL[31] and on pulse lines at Cornell University. The radially converging feeds described previously in the Proto II generator[18] are also transformers.

E. Beam Diodes

In the previous sections we have outlined design criteria for the production of short-duration high-power pulses. To convert these pulses to particle beams requires the use of a high-voltage, low-inductance diode. Two diode arrangements are illustrated in Fig. 7. In the first of these figures we show a stacked-ring insulator in which the lucite insulating rings are alternated with annular aluminum discs. The lucite insulators are typically cut, on the vacuum side, at 45° to the axis of the diode and arranged so that electrons leaving the surface of the dielectric do not hit the plastic, causing secondary emission and a subsequent breakdown. The aluminum disks serve as grading rings, distributing the diode voltage uniformly along the length of the insulator. If the surrounding dielectric is water, this grading of the fields may be very effective. For oil insulation, the ring-to-ring capacitance is reduced and the field distribution is less uniform. In this case, the rings still serve the purpose of breaking the path of any incipient surface flashover. This type of diode has been satisfactorily used for a variety of electron-beam machines and can be safely stressed to about 150 kV/cm. A variation on the design is shown in Fig. 8. This variant is in use as a double-diode system for pellet-fusion applications. In such application, a very low diode inductance is required

† The switch rise time will be, for a given line impedance Z, greater in the geometry shown in Fig. 5, than for the arrangement in Fig. 4b. The arrangement in Fig. 4b may be preferable in low-impedance lines.

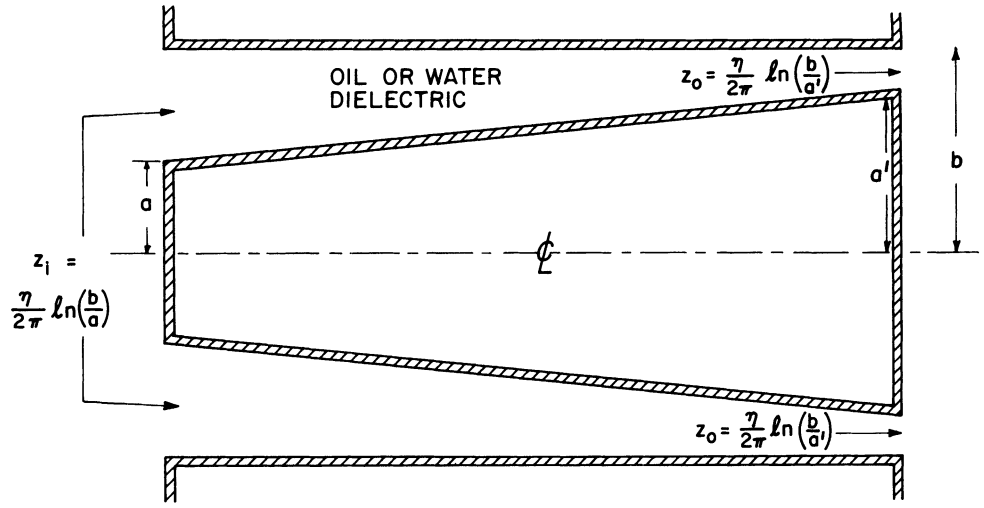

FIGURE 6 Section of a coaxial transformer. The line impedance varies adiabatically along the length of the system from Z_i at the input to Z_0 at the output.

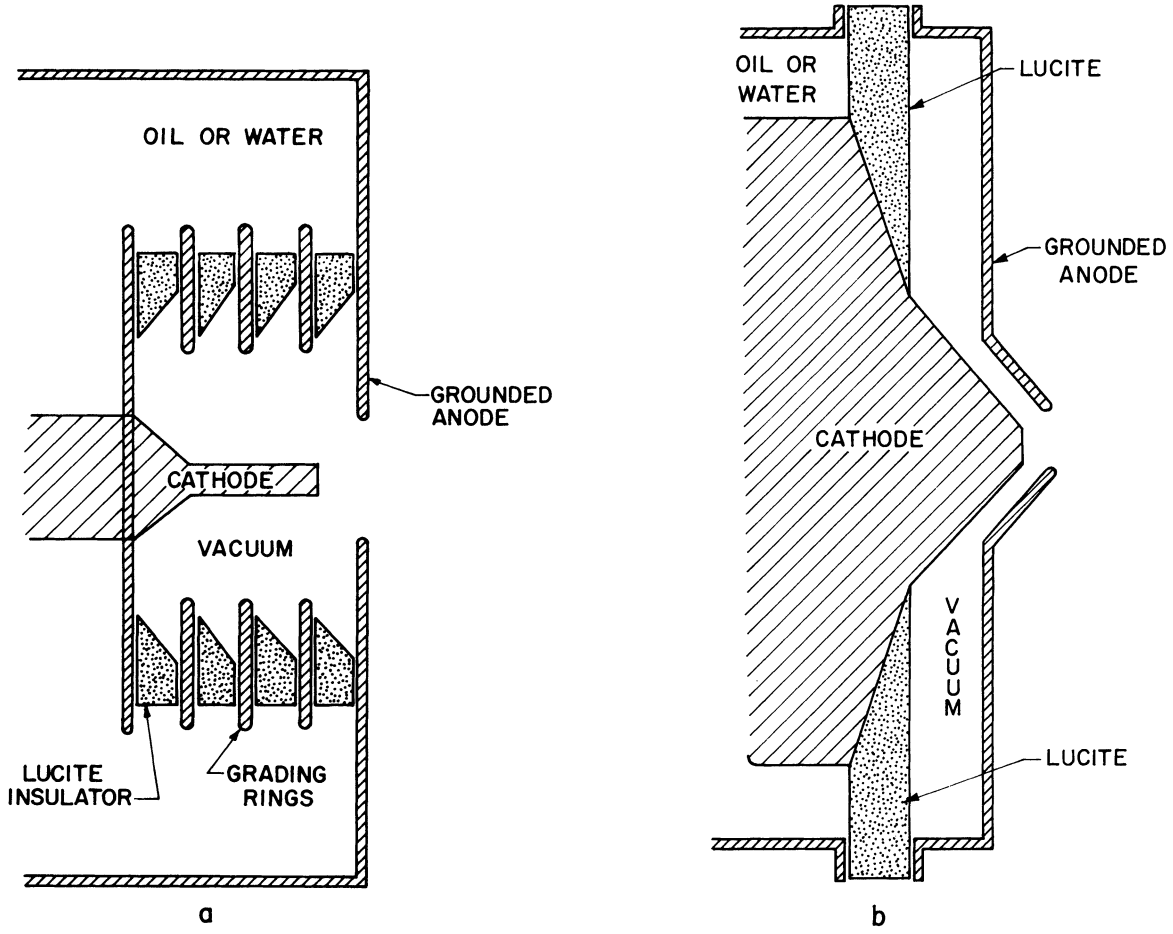

FIGURE 7 Vacuum diode assemblies using: a) a graded ring assembly, and b) a single radial insulator.

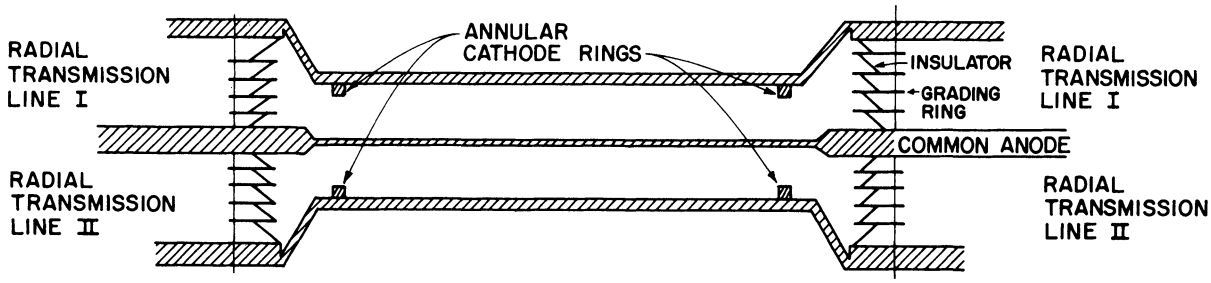

FIGURE 8 Two-sided diode used in pellet fusion experiments. High current electron beams emitted from the annular cathodes self pinch to the axis of the system. The system is fed from both sides by two similar transmission line systems.

and is achieved, using the geometry shown, with electron-beam emission occurring at large radii, close to the insulator rings. It is worth noting that the limiting electric-field stress at the diode rings, coupled with the radius of the rings, leads to a limitation on the generator current delivered to the load. In a uniform strip transmission line, the current flow per unit width of the line is given by

$$I = \frac{E\sqrt{\varepsilon_r}}{377} \ A/m. \qquad (14)$$

For the lucite-ring assembly illustrated in the previous figure, the current capability of a two-sided 1-m radius diode, at a safe maximum stress, is about 0.75 MA, corresponding to a power flow density of about 0.1 GW/cm^2. The total power flux into the diode is too small for pellet-fusion applications[12] and it is necessary to go to magnetically insulated feeds to increase the power flow to the target. A promising approach to this problem is under investigation in both the U.S.A. and the U.S.S.R. It employs magnetic insulation of transmission lines.[38-41] This will be briefly indicated later, following the discussion of ion-beam generation.

A second diode configuration using a single insulating structure without grading has been extensively used at NRL and in other laboratories.[29,31] The insulator configuration is illustrated in Fig. 7b. In this design, considerable effort is devoted to forming the electric-field lines at large angles to the dielectric interface, so that any electron emitted cannot hit the insulator surface. Design figures of 315 kV/cm have been quoted for flashover on lucite at large angles, and the VEBA machine at Naval Research Laboratories has been operated at maximum field stresses of about 220 kV/cm. In addition to requiring that the electric-field lines make a large angle to the plastic interface, care is also taken to ensure that triple points, such as that occurring at the junction of a lucite wall with metallic wall and a vacuum are buried and not directly visible along the dielectric interface. The electrical stress is also minimized at these junctions. The detail of the buried junction is omitted in Fig. 7. The 'O' ring seals in metallic-dielectric interfaces are usually buried in the metal surface.

III. ELECTRON AND ION BEAM GENERATION

The diode configurations used in beam generators have been illustrated in Fig. 7. The beam generation depends, of course, on the polarity of the generator used in pulsing the diode. We describe initially the operation of a diode as an electron-beam generator, and subsequently outline the modifications used for the generation of ion beams. In both configurations, the vacuum used is quite modest and typically in the range of 10^{-5} to 10^{-3} Torr.

A. Electron-Beam Generation

The mechanisms associated with electron-beam generation in moderate-size electron-beam generators were studied in detail by Parker et al.[42] They operated an accelerator capable of generating an electron beam with an impedance of a few ohms at voltages in the three to four hundred kilovolt range. Typically, carbon cathodes were used as the electron source and the beams were extracted through a thin anode foil. With cathode diameters of about 5.0 cm, anode cathode gaps of a fraction of a centimeter were used to generate the beams. The applied voltage pulse was found to precede significant current flow by a few nanoseconds. During this phase, the current emission occurs through field emission from whiskers protruding from the cathode surface. The probable current density is limited to a few amperes per square centimeter during this phase, corresponding to field enhancements at the

whisker sites in excess of 100. As the enhanced field approaches a value of about 10^8 V/cm, the whisker current increases to provide sufficient energy to cause volatalization of the whisker tips. Subsequent emission comes from the plasma formed by the ionization of the vapor surrounding the cathode. This current may be quite large and is found following completion of the first phase of breakdown. The emission from the plasma approximately satisfies the Child-Langmuir relation for the diode geometry, provided that account is taken of the closure of the diode gap by the expanding cathode plasma. Observations made by Parker et al. and other groups[43] show that plasma-front velocities of one to four cm/μsec occur. As the beam current is increased, absorbed gases at the anode are released and ionized. A further plasma front originating from the anode starts to close the diode gap and the diode perveance increases further. The anode–plasma front velocity is less than that for the cathode plasma and usually about 1 cm/μsec. The flow is reasonably uniform from the diode unless significant field enhancements are present due to edge effects on the electrodes. The beam 'temperature' has been determined in a number of laboratories and found to be largely controlled by the scattering of the electrons in transit through the anode foil. Electron beams with energies in the range centered around 0.5 to 1.0 MeV have been obtained with mean scattering angles of a few degrees.

The presence of a preformed plasma in the diode, either from prepulse effects or due to plasma injection from an external source leads, in the case where the plasma density is high, to a rapid collapse of the diode impedance and to a shorting of the generator. Miller et al.[44] have shown that if the plasma density is limited to the 10^{13}–10^{14} cm^{-3} range, then the diode shorting does not occur and the diode behaviour can be well described by laminar bipolar flow. The current density is found to satisfy the equation

$$J_E = \sqrt{\frac{M_p}{m_e}}\, J_p, \tag{15}$$

where

$$J_p = 1.86 \left(\frac{4\varepsilon_0}{9}\right)\sqrt{\frac{2e}{M_p}}\, \frac{V^{3/2}}{x^2}, \tag{16}$$

and x is the thickness of the plasma sheath. The ion-current density is given by the usual bipolar flow limit, provided that proper account is taken of the expansion of the plasma sheath to allow for the provision of an adequately large flux of ions. This effect was important because the ion saturation current was typically less than that permitted by the space-charge-limited Child-Langmuir law.

Electron-beam generation has also been accomplished in foilless diodes. In cases where the electron beam is to be propagated in vacuum, such as in microwave-generation experiments or in some collective-acceleration systems, the practically obtainable beam impedance is high and can be achieved from a foilless diode. A beam propagating in vacuum along a strong magnetic guide field, has a space-charge limiting current given by[15,16]

$$I_L = \frac{17{,}000\,(\gamma^{2/3} - 1)^{3/2}}{1 + 2\ln\left(\frac{b}{a}\right)}, \tag{17}$$

where a and b are the beam and tube radii respectively, and γ is the relativistic factor for the beam electrons at the anode plane. This value has been confirmed experimentally.[17] Other equilibria, in finite magnetic fields, in which the electrons rotate around the beam axis, have also been determined.[45,46] These also represent high-impedance beams.

Two foilless-diode configurations have been employed for the generation of electron beams. These configurations are sketched in Fig. 9. The first configuration[47] is essentially a magnetron type gun, in which the electrons are injected across the guide magnetic field. The magnetic field is sufficiently strong that the electrons do not cross the diode gap, but rather 'drift' into the experimental region following the curved magnetic-field lines. The second configuration is designed to inject the electrons approximately parallel to a uniform guide field.[14] In this configuration the electrons usually pass within a gyroradius or two of the anode plate. Both configurations are especially suited to high-impedance applications where a repetition rate or vacuum application is involved.

We now continue the discussion of foil-diode systems with a review of beam-pinching processes. As the diode current is increased, conditions develop which permit the beam to pinch as a result of the $\vec{J}\times\vec{B}$ interaction between the self magnetic field of the beam and the electron current. Pinching occurs when the current exceeds a critical current determined from the relations

$$\frac{I}{I_A} = \frac{\nu}{\gamma} \approx \frac{r}{2d}. \tag{18}$$

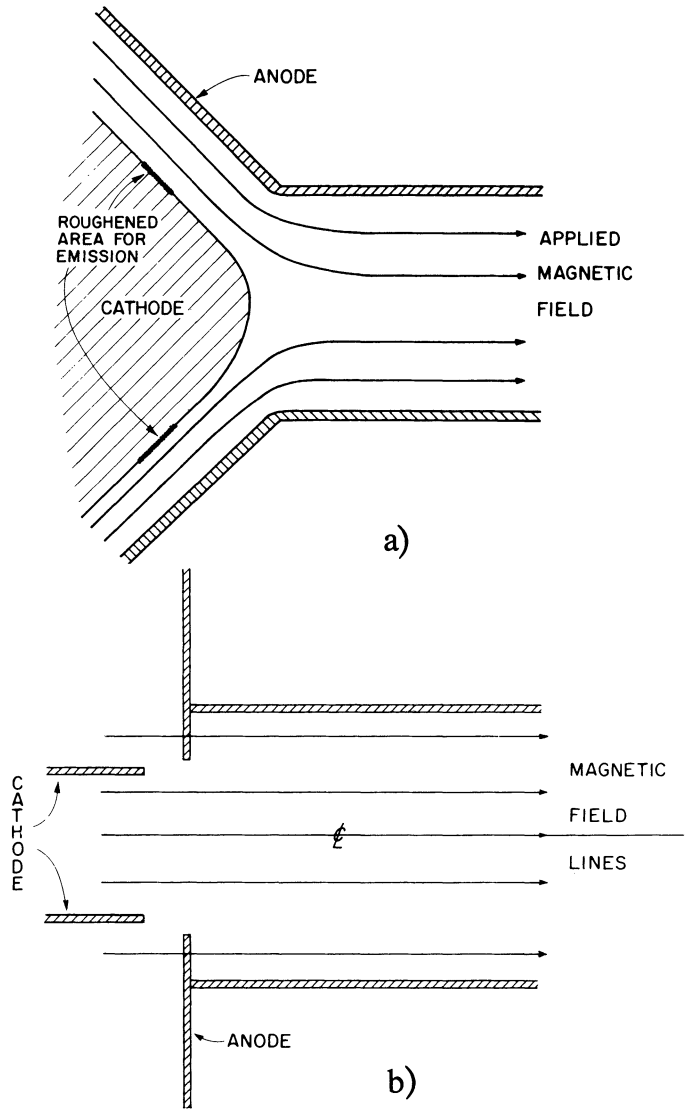

FIGURE 9 a) Foilless diode in which emission occurs orthogonal to the applied magnetic guide field. b) Foilless diode in which emission is parallel to the magnetic field lines.

In this relation ν is the number of electrons per classical electron-radius length of the beam and γ is the usual relativistic factor. The diode electrode gap is d and the cathode radius is r. The ratio ν/γ is also frequently designated as I/I_A, where

$$I_A = \frac{4\pi\varepsilon_0 m_e c^3}{e}\beta\gamma = 17{,}000\,\beta\gamma \quad (19)$$

is the Alfven-Lawson limiting current. The above relation [Eq. (18)] determines the value of the electron-beam current at which one expects non-laminar flow to develop.[48] Equation (18) may be simply derived by equating the gyroradius of an outermost electron in the beam to the diode-gap d. When these parameters are equal, one expects to find significant self-pinching of the electron beam. This result has been shown to give a reasonable account of the threshold for self-pinching, provided that one uses the actual diode spacing in the estimate, i.e., after allowance has been made for the gap closure of the plasma fronts from the cathode and anode plasma.[49]

Diode pinching is of considerable interest, since it has application to controlled-fusion pellet heating. Considerable analytic theory and simulation[50–54] have been carried out to determine optimum conditions for maximum compression of the electron beam. Qualitatively, it has been found that diode pinching always occurs when the diode current exceeds the value given in Eq. (18), although the pinch may not always be symmetric about the diode axis or always collapse to a very small radius. Important processes in determining the degree of the diode pinching and its control include the provision of a plasma on the axis of the diode (produced, for example, by an exploding wire) to neutralize the space charge of the beam in the late stages of collapse and, more importantly, the role of positive ions formed at the anode of the diode in determining the orbits of the electrons as they collapse to the axis. Other attempts to produce high current densities on the axis include the work of Morrow et al.,[55] who found that current densities in excess of 1 MA/cm^2 could be achieved on axis when a thin dielectric-rod cathode was used as the beam cathode. These results were subsequently confirmed by Condit et al.[56] and by Bradley and Kuswa.[57] The utility of this technique appears to be restricted to relatively high-impedance ($\lesssim$ 20 ohms) diodes; it did, however, stimulate the interest in electron-beam pellet fusion in pulsed-power generator diodes.

A satisfactory configuration used in the production of tightly pinched beams employs a hollow cathode which has a radius R much larger than the diode cathode–anode gap d. Simple theoretical models have been formulated for this configuration to describe the pinch characteristics. Both of the models presented predict that the diode current will have a magnitude given by a relation of the form

$$I = 8{,}500\, g\, \gamma \ln[\gamma + (\gamma^2 - 1)^{1/2}], \qquad (20)$$

where the parameter g depends on the details of the diode geometry. For the annular cathode $g = R/d$ in the parapotential flow model, and $g = R/d(\gamma)^{1/2}$ in the focused-flow model. The parapotential flow concept, which is originally due to dePackh[50] has been extended by Creedon.[51] In parapotential flow, one deals with a class of exact analytic solutions for the flow of electrons along equipotentials. In such a flow the rate of change of momentum of the electrons is zero and $E = -\boldsymbol{v} \times \boldsymbol{B}$; the electrons then drift under the influence of the $\boldsymbol{E} \times \boldsymbol{B}$ force, with zero Larmor-radius orbits, along conical paths from the cathode to the anode. The parapotential flow model does not address the problem of the connection of the region of parapotential flow to the anode or cathode regions of the diode. Equation (20) describes the relation for saturated parapotential flow, in which the flow is focused along an equipotential terminating on the anode surface. The focused-flow model,[52] which exhibits an identical dependence (apart from the factor $\gamma^{1/2}$ in the relation for g) on the diode voltage to the parapotential flow, results from an integration of the cold-fluid electron model equations through the diode. In this model, the presence of a plasma at the anode and cathode surfaces plays an important role in determining the pinch. The flow may be represented largely as an $\vec{E} \times \vec{B}$ drift of the electrons through the vacuum region of the diode. The degree of pinching in this region is relatively weak. The final pinching is achieved in the charge- and current-free anode–plasma environment. Due to the similarity in the expressions for the current dependence on the diode voltage, many of the basic characteristics of both models have been confirmed.[58–60] For example, in the energy range extending from about 0.5 to 1.0 MeV, the diode impedance is essentially independent of the voltage, as has been observed experimentally. There are differences between the models, however, and their predictions do not coincide. An important difference is that the focused-flow model requires the presence of a plasma (or at least a counterstreaming ion flow) in order to produce the final stage of the pinch flow. This anode plasma has been shown to play an important role in determining the final stages of the compression. Cooperstein and Condon[60] have found that the empirical relationship

$$I = 8{,}500 \left(\frac{R}{D - \Delta}\right) \gamma^{1/2} \ln[\gamma + (\gamma^2 - 1)^{1/2}] \qquad (21)$$

provides a satisfactory description of the diode behavior. In their experiments, an effective diode-gap reduction Δ was identified as 0.15 cm, about 40% of the actual gap, and was independent of time. A possible explanation of this is associated with the large self magnetic field of the beam following the pinching, inhibiting the further expansion of the anode plasma. It should be noted, however, that the focused-flow model is strictly applicable for solid-cathode configurations and for a steady-state current flow following the pinch completion.

Subsequently detailed study of the time dependence of the pinch collapse in the annular-cathode configuration lead to an important realization, namely that the anode plasma sheath could not adequately account for the initial formation of the

pinch. Following application of the diode voltage pulse across the gap, an annular beam described by the Child–Langmuir equation is formed. As the current exceeds the critical current for pinching, a weak pinch is initiated. The impact of the beam electrons on the anode produces a plasma which expands towards the cathode with a velocity of about 2 to 4 cm/μsec. This expansion rate is insufficient for the formation of the plasma sheaths which are needed to obtain electron focusing on the axis. This realization resulted in a re-examination of the previous models and led to a new model in which the plasma at the anode served as an ion source for bipolar flow in the gap.[61–65] Once the critical current is exceeded and pinching starts, positive ions from the newly formed anode plasma stream towards the cathode. This flow enhances the diode electron current due to the redistribution of space charge in the gap. In its turn, the enhanced electron current helps augment the pinch compression. In this model, the radial pinch time is limited by the ion flow time through the gap. The characteristic ion velocity is more than two orders of magnitude greater than the corresponding plasma expansion rate; hence the diode pinch can develop rapidly. Radial collapse rates for the electron-beam pinch of up to 5 mm/nsec have been recorded experimentally. By varying the anode material, it has been shown that the radial collapse velocity of the pinch is dependent on the heating at the anode and hence on the release and subsequent ionization of the absorbed gases in the anode material.

B. Ion-Beam Generation

As noted in the previous section, bipolar ion and electron flow occurs in high-current beam diodes. Elementary calculations show that in space-charge-limited bipolar flow, the electron-beam current is enhanced by a factor of 1.86 over the pure electron flow. With allowance for relativistic effects, this enhancement may exceed a factor of two and has been calculated to rise to 2.14 at 5.0 MV.[66] Energy transfer to the ions (which unless otherwise stated will be taken to be protons) is limited, nonrelativistically, to the square root of the electron-to-ion mass ratio, namely 2.3% for protons.

Following the work of Humphries et al.,[67–69] a considerable effort has been devoted to developing proton sources with about 1-MeV energy, comparable to the high-current electron sources described previously.[70–73] This work has been largely motivated by the particle-beam pellet-fusion concept. High-current proton beams with energies in the one to ten megavolt range are particularly attractive for this application, since all energy deposition in the target is classical. In addition, ion-beam research is aimed at producing adequate proton fluxes to generate a field-reversed layer for magnetic confinement of thermonuclear plasmas.[3,14,74–76] To preview the following discussion we report that substantial progress has been made in this direction; sources available at present have achieved powers of about 0.7 TW at proton energies of about 1 MeV.

The principal effort in the production of high-current ion beams has been centered on the development of techniques for the suppression of the unwanted electron flow. Three main methods or devices have been developed to suppress the electron current, namely: a) the reflex triode and tetrode; b) magnetically insulating diodes; and c) pinched-beam configurations, in which the electron beam impedance is increased due to the long electron path in crossing the diode gap. We now examine these approaches in more detail.

The reflex triode was the original configuration used in the study of intense proton-beam generation by Humphries et al.[67,68] In this device, which is shown schematically in Fig. 10, the electron-current flow is suppressed and the ion current flow correspondingly enhanced by reflexing the electrons through the anode. In order to transfer energy efficiently to the protons, it is necessary to suppress the electron flow. In the reflex triode, the electrons emitted from the cathode traverse the diode gap and subsequently see a reverse field which tends to decelerate them. In practice, the center (anode) electrode is pulsed positively and hence the potential hill encountered by an electron, which has traversed the first part of the diode, is sufficiently large that the electron will be reflected at or close to the plane of the second cathode. In contrast to this, an ion formed at the anode plane will fall through the diode potential well, and, provided that the cathode is transparent, will emerge from the back of the cathode. The situation sketched in Fig. 10a is symmetric about the anode plane and hence the maximum efficiency which can be achieved in this configuration is limited to 50%. In practice, there is no need to use a second cathode electrode because the space charge beyond the anode will ensure the formation of a virtual cathode, and hence provide the reflexing of the electrons required to allow the ion flow to dominate.

There are a number of additional criteria that must be met before one can satisfactorily produce an ion beam from a reflex triode. The foremost of these

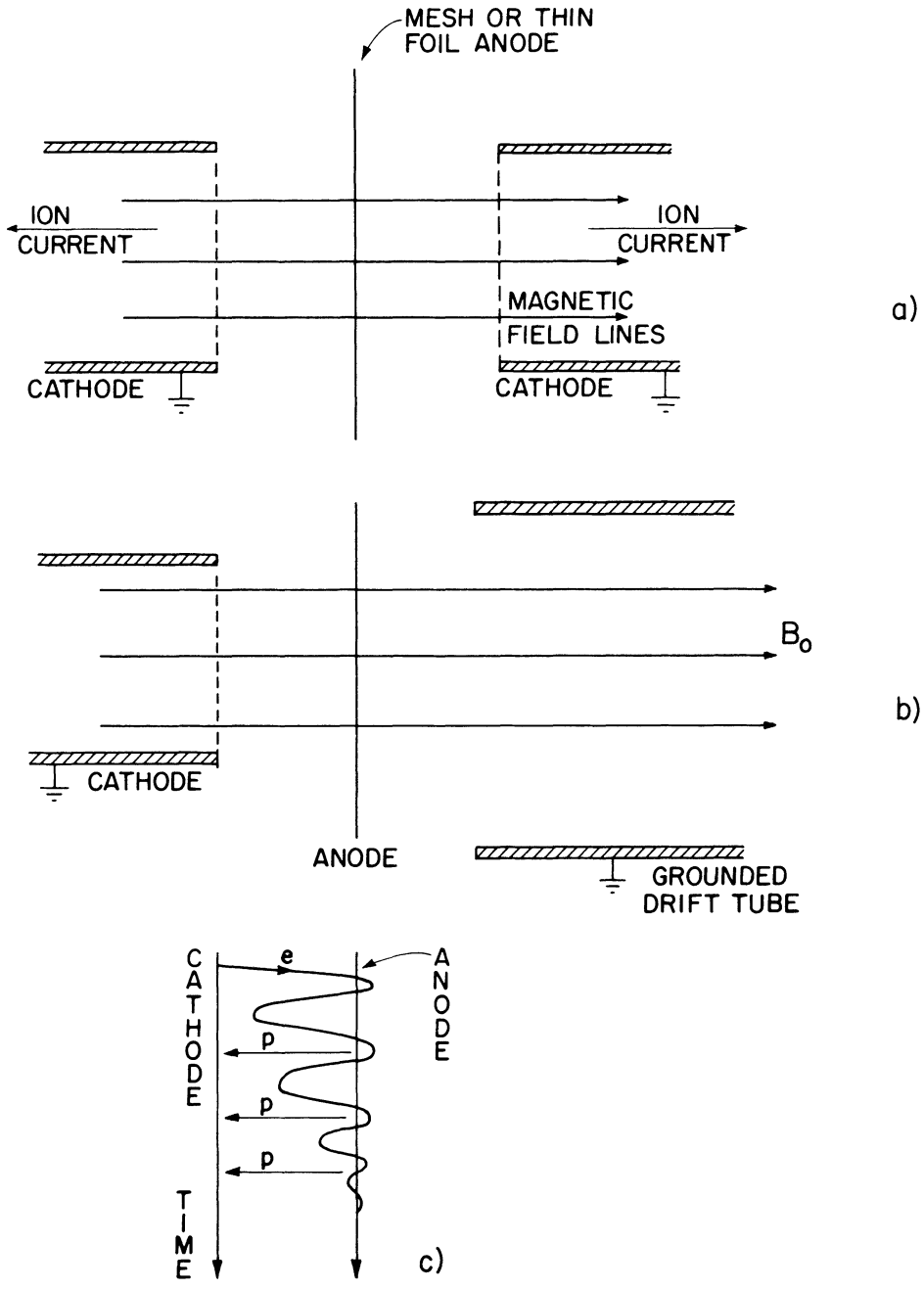

FIGURE 10 a) Reflex triode with two real cathodes. b) Reflex triode with one real and one virtual cathode. c) Trajectory of an electron through the reflex triode b. Energy loss in the anode foil leads to eventual loss of the particle in the foil. Protons only make a single traverse of the diode gap.

is concerned with the maintenance of at least a quasi one-dimensional configuration for the electron flow. The accumulation of negative space charge in the diode region will lead to the development of a radial electrostatic field which tends to expel the electrons from the diode region. This may be prohibited by a sufficiently strong axial guide magnetic field. Typically fields of order 10 kG are used in practice,

although several experiments have been satisfactorily carried out with the guide fields as low as about 1.6 kG.[71] An additional complication encountered with the reflex triode is the tendency of the diode gap to short due to gap closure arising from the plasma motion across the diode gap. We therefore find that diode gaps tend to be larger in ion-generation experiments than one would find in corresponding electron-beam generators. The Child–Langmuir space-charge-limited current flow from an evacuated diode, in which the electron current has been suppressed, is only slightly greater than two percent of the current obtained in the electron mode. Hence we find that large-area cathode configurations are appropriate for high-current applications.

The theoretical basis for the reflex-triode system was developed by Antonsen and Ott[78] and indepenently by Creedon, Smith, and Prono.[79] In both of these approaches a thin foil anode was considered. Multiple scattering of the electrons in the anode foil leads to an increase in the number density of the electrons close to the anode. The enhanced electron density in this region gives an increase in the ion emission from the hot anode plasma. A scaling study of the dependence of the ion current density on the diode voltage reported that current densities of up to 200 A/cm^2 were achieved, compared with the 30–50 A/cm^2 in the original mesh-anode studies. In addition, it was observed that the emitted current scaled much more rapidly with the diode voltage than the three-halves power law anticipated.[71,80] Ott and Antonsen showed in their analysis that the ion to electron current-density ratio could be described by a relation of the form

$$\frac{J_p}{J_e} = (1+\nu)\left[\frac{Z_m}{M_p}\right]^{1/2}, \qquad (22)$$

where ν is a constant given by

$$\nu = 2\,\frac{(1+\ln 4)}{3\langle\Delta\theta^2\rangle} \qquad (23)$$

In these relations Ze is the charge on the ion and $\langle\Delta\theta^2\rangle$ is the mean square scattering angle. Kapetanakos et al.[71] point out that the scattering angle term is approximately inversely proportional to the square of the diode voltage. Assuming a three-halves power law for the electron current density, we conclude that the ion current density should scale rapidly with the diode voltage. In this estimate the dependence is seen as a seven-halves power of the diode voltage. While the detail of the scaling is not clear, it is apparent that the ion current density does scale more rapidly than expected on the basis of the Child–Langmuir law and further that a thin foil anode leads to a greater ion current than one can achieve with a solid anode. The largest reported proton flux densities correspond to current densities of about 3 kA/cm^2.[72]

A recent development of the reflex triode has lead to a further increase in the available current density.[8] To achieve this, a second anode foil has been used. The reflex tetrode, which is sketched in Fig. 11, shows two anodes: the first, which is labeled A1, is constructed from Polycarbonate or aluminized Mylar. Previous experiments had established that both of these materials are poor proton emitters. The purpose of this configuration is to limit the proton flux towards the cathode, and to provide a good ion source at the second anode A2. The ion flux from the second anode must flow in the direction toward the virtual cathode, since the electrostatic field between the two anode planes is zero. The results obtained with this configuration show that an increase in the current densities obtained is consistent with single-direction ion flow. In these experiments a conversion efficiency, defined as the ratio of the extracted ion current to the total generator current, of up to 55% was achieved. To achieve this efficiency, it was necessary to use a thin foil (2 μ Polycarbonate) for the first anode and to optimize the anode separations. In the work described, the optimum separation was found to be about 0.5 cm. The results were insensitive to the guide-field strength in the range (2.7 to 7.6 kG) used.

The work on the reflex-triode system was closely followed by the study of magnetically insulating diodes.[82–93] The underlying principle of this device is

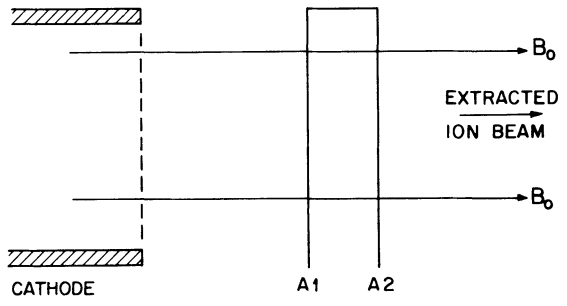

FIGURE 11 Schematic showing the principle of the reflex tetrode. The first foil A1 is a two micron polycarbonate sheet and is separated from the second anode A2 by about 0.5 cm.

shown in Fig. 12. A transverse magnetic field is applied across the diode. The field is sufficiently strong that the electrons will execute magnetron-like orbits and not be able to reach the anode plane. Calculations give the required field strength to produce magnetic insulation as approximately[77,88]

$$B_{cr} = \sqrt{\frac{2\,m_e V}{e}}\,\frac{1}{d}\left[1+\frac{eV}{2m_e e^2}\right]^{1/2}. \quad (24)$$

In crossing the diode gap, the protons are also deflected, but, due to their greater mass, their deflection is quite small and is readily shown to be of order

$$\bar{\theta} \sim \sqrt{\frac{m_e}{M_p}}\,\frac{B_0}{B_{cr}}, \quad (25)$$

where B_0 is the insulating magnetic field and B_{cr} is the critical field to achieve magnetic insulation. The angular deflection is of order one to two degrees and, if important, can be compensated by application of a magnetic field subsequent to proton extraction through the cathode plane.

A measure of the success of an insulating diode is the reduction in perveance of the diode as the field exceeds the critical field. Typical results,[93] with a copious source of plasma at the anode, are shown in Fig. 13. The perveance approaches the ion space-charge limiting value as shown by the dashed line, provided proper account is taken of the reduction in the diode gap spacing due to the space-charge neutralizing effect of the electrons emitted from the cathode.

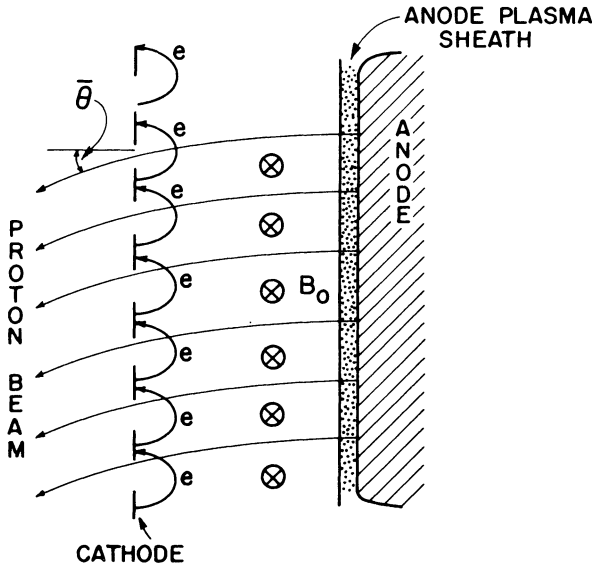

FIGURE 12 Schematic showing the principle of the magnetically insulated diode. Protons, emitted from the anode plasma, traverse the diode gap emerging through the cathode at a mean scattering angle $\bar{\theta}$ to the diode axis. The electron motion is cycloidal along the cathode with electron flow inhibited by the traverse magnetic field B_0.

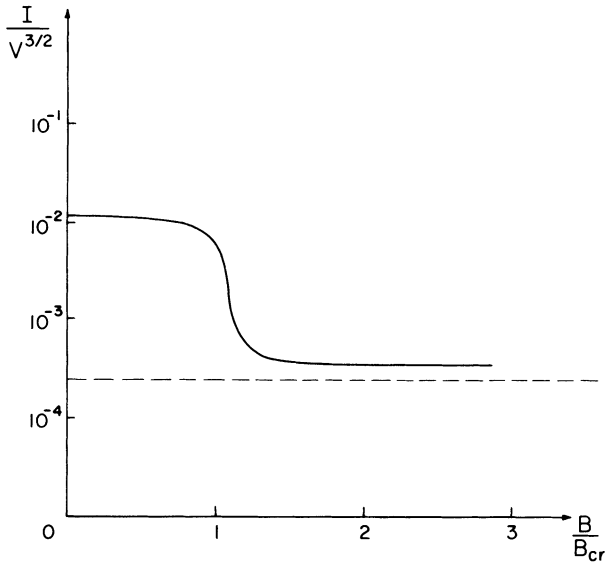

FIGURE 13 Reduction in diode perveance as a function of the magnetic field strength. This figure is based on data presented by Greenspan et al. [*Phys. Rev. Lett.* **39**, 24 (1977)].

There are two essential requirements for satisfactory operation of a magnetically insulating diode, a copious and prompt supply of ions at the anode plane, and a well-designed magnetic-field configuration. The former problem has been largely solved using surface-flashover techniques similar to those used for many years with plasma cathodes. In essence, a plasma is formed on the electrode, due to the electrostatic breakdown of the surface of a dielectric inclusion in an otherwise conducting plane. The rapid risetime of the applied potential requires the electric-field lines to follow the metallic anode surface. This results in the formation of electric fields along the surface of the dielectric inclusions. The breakdown along the dielectric surfaces produce the required ion-plasma source. Since most plastic dielectrics are hydrogen-rich, and since protons are the lightest of the ions, the preferential emission is protons.

The magnetic-field configuration required to produce the magnetic insulation is more complex, since one requires that the field lines do not cross the diode

gap. In practice, some field lines will almost always traverse the gap but their effect need not be too serious if the path length of the field lines in crossing from the cathode to the anode is much larger than the direct anode–cathode separation. Practically, this means that the field must not allow the electrons to easily traverse the gap so that they can absorb the generator power.

Various configurations have been used in magnetic-insulation experiments, although in much of the published work, two concentric cylinders with the cathode as the interior electrode have been employed. In these experiments, the ion beam is frequently extracted through holes in the cathode surface. In these experiments attempts have been made to focus these protons on to a line focus and current-density increases of an order of magnitude over the density at the cathode have been achieved. Similar studies have also been made recently using sections of a sphere for the anode and cathode to obtain a point focus for the ion beam.

Luckhardt and Fleischmann[85] have used magnetic insulation to produce long-duration proton pulses. In their experiments, a strong 20-kG magnetic field was used to insulate a 300-kV diode, consisting of two concentric cylinders, for times of up to 4 μsec. Two important results were noted; first in long-duration diodes the ion current achieved could exceed by a factor of order ten the predicted space-charge limiting emission based on the initial diode geometry, and secondly, high total numbers of ions could be generated. This latter result has application in the generation of field-reversing layers where the total number of particles generated is important. The ion yields reported are approximately ten times greater than those obtained with short-pulse machines operated under comparable diode-voltage conditions. Extension of this work[86] to megavolt energy has produced ion beam-current densities of up to 300 A/cm^2 for 1 μsec.

Magnetic insulation has been shown to provide a useful means for the generation of intense ion beams. The techniques developed have the additional advantage that they do not lead to a destruction of the anode with each event. The emitted current density is, however, still somewhat lower than that reported for reflex triodes. Typical peak current densities achieved to date are about 100 A/cm^2 with short-duration pulses and up to 300 A/cm^2 in long-pulse systems.

Although it is somewhat out of place to describe magnetically insulated transmission lines in the discussion of ion diodes, it is appropriate to point out that the same insulation process has been used to achieve the extremely high power-flow densities required for electron-pellet fusion. As pointed out earlier, the dielectric-strength properties of diode insulators limit the current and hence the power flow [see Eq. (14)] from the generator to the pellet. This limitation has been identified as a primary obstacle in the power-flow analysis. A successful solution to this problem has been found using the self magnetic insulation of vacuum transmission feeds.[38,41,94–99] At sufficiently high current levels, the self magnetic field of the transmission line wave is adquate to produce magnetic insulation. The best results achieved for power transfer have used a 7-m long triplate vacuum feed at electric-field strengths of up to 7 MV/cm.[99] This represents an increase of approximately 50 over the stress limits set by plastic diode insulating rings. About half of the power flow occurs in the vacuum fields along the vacuum line. The parapotential flow theory[51] is also relevant in this regime.

The final approach to be described in the generation of intense ion beams uses the self-pinch properties of electrons in vacuum diodes. This process has been extensively studied in various laboratories and also in computer simulation stud-

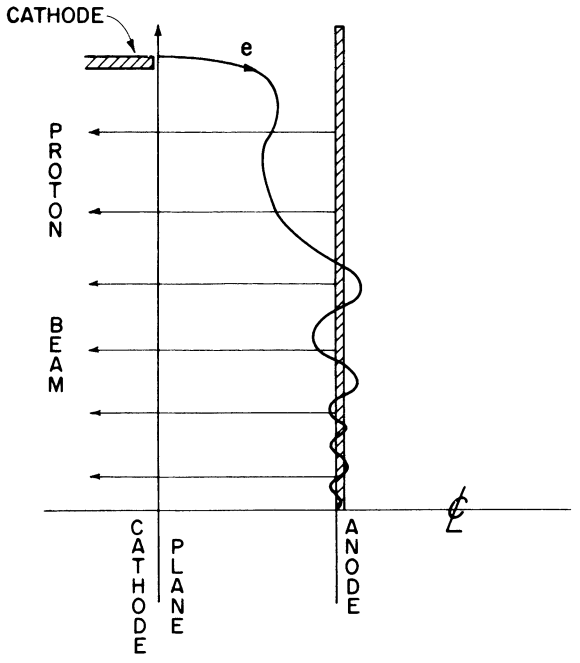

FIGURE 14 Ion and electron trajectories in a pinched electron beam diode. A thin anode foil is assumed.

ies.[64,100–107] The essential feature of the ion-beam generation is sketched in Fig. 14. Consider the production of a pinch beam using a large aspect-ratio diode with an annular cathode. The electron flow is initially laminar. As the current increases, the energy absorbed in the anode due to the electron-beam bombardment increases and eventually results in the release of gases and in the formation of a plasma in the anode material. The plasma formed drifts across the diode gap at a velocity of order 1 cm/μsec and is preceded by ion flow. The bipolar flow in the diode causes the electron-beam current to increase and beam pinching commences. At each stage of the compression, more plasma is released from the anode, ion emission from the plasma is established and the electron-beam pinch continues. When the electron beam reaches the axis of the diode, we achieve a quasi-steady state in which the electron current follows a long path from the cathode edge to the axis, while the ion emission follows an almost straight line path from the anode to the cathode. It has been shown that the difference in particle paths leads to a substantial increase in the energy transfer to the protons. The estimated ratio of ion to electron currents has a value[64]

$$\frac{I_p}{I_e} \gtrsim \tfrac{1}{2}\left(\frac{R}{v_e}\right)\left(\frac{v_p}{d}\right) = \frac{R}{2d}\left(\frac{2\text{ eV}}{M_p c^2}\right)^{1/2}, \quad (26)$$

where v_e *and* v_p are the final electron and ion velocities. For values of the aspect ratio $R/d \gg 1$, it is possible to achieve approximately equal ion and electron currents. More detailed numerical simulations have shown that this ratio can reach a value as high as three. Stephanakis et al.[102] have reported obtaining 4×10^{16} protons over 120 cm^2 from the Gamble generator. Of the 0.5 to 0.6 MA of current, about 150 to 200 kA was attributed to the protons.

A detailed study of the pinch process was carried out by Swain et al.[108] using a 200-kV, 50-kA generator. They observed that with a solid aluminum target 1 to 3 kJ/g of energy was required to generate the ions, and that with hydrocarbon anodes this figure could be reduced by about one order of magnitude. Irrespective of the anode material and its treatment, the primary ion found was either H^+ or H_2^+ and was presumably due to the rather poor vacuums usually used in high-power beam diodes ($\sim 10^{-4}$ Torr). In their investigation, they reported that all the ions observed had an energy approximately determined by the diode voltage and that ions with mass to charge ratio of 1, 2, 6, 12, and 16 were obtained. The maximum recorded current density for the protons was about 1 kA/cm^2. Unpublished studies at Cornell[109] have found that heating the anode foil, while under vacuum, to red heat causes an increase in the diode impedance by a factor of up to two. Presumably this is due to a reduction in the hydrocarbons absorbed on the foil from the pump oil and vacuum grease.

As might be anticipated from the discussion of the reflex triode work, the pinch process has been found to be helped by using thin anode foils[102,104] instead of solid targets. The reflexing of the electrons then results in an enhanced electron density close to the foil and a corresponding build up of the proton current. This is accompanied by a more rapid pinching of the electron beam. It is worth noting that the rise time of the ion beam is comparable to the collapse time of the electron pinch and that occurs on a time scale much shorter than the electron-beam rise time. Efforts to aid diode pinching by the use of an externally driven axial[110] diode current did not lead to an improvement of the diode pinch process, which seems to be primarily controlled by the proton emission from the anode surface. Exploding wires have also been used to produce a plasma on axis for space-charge neutralization and to aid focusing.[111]

D. Repetition Rate

Primary interest in high-power electron and ion beam generators has been centered on low-impedance, very high power devices. To date, none of these devices has been operated with a repetition rate greater than a few pulses per hour. To demonstrate the feasibility of such an accelerator, work has been carried out at Sandia on the use of a modest accelerator in a repetition-rate mode.[112] A 350-kV, 300-J accelerator has been pulsed at a repetition rate of 40 pulses per second for over a million successive shots. For a short period operation was maintained at 100 Hz.

IV. INDUCTION ACCELERATORS

As stated early in this review, relatively little work has been done on utilizing pulsed-power technology to obtain very high-energy, medium-current relativistic beams.

The first devices used for this purpose were the electron linear-induction accelerators built at LBL,[113] LLL,[114] and NBS.[115] The essential features of an induction linac are shown in Fig. 15. In this device, the center conductor is pulsed negatively from a pulse or Blumlein transmission line. The

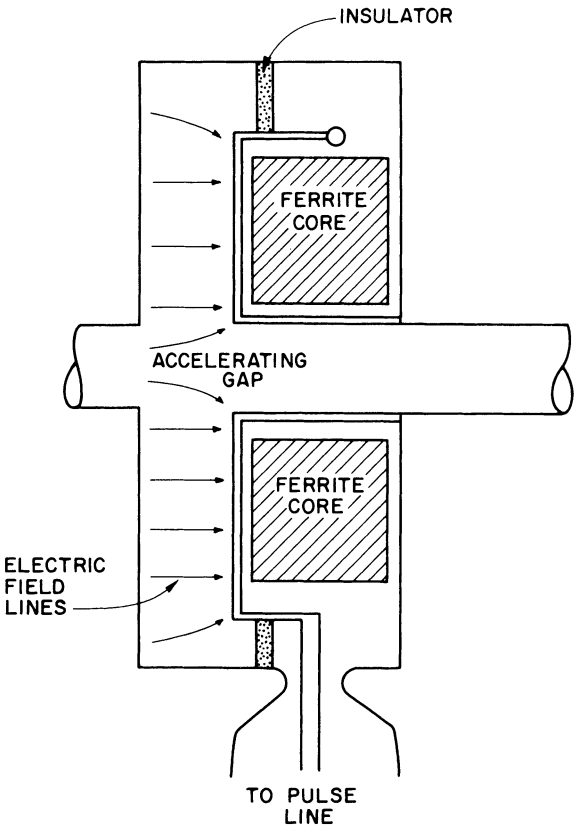

FIGURE 15 Induction assembly acceleration module. The field lines are appropriate for positive ion acceleration from the left to the right.

incoming wave divides between the two halves of the system with each half feeding a section of a cylindrical ferrite core which surrounds the beam channel. The induction field appears concentrated across the accelerator gap. Following acceleration of the electrons through the gap, they are buried inside a hollow pipe in which the electric field is zero. Following a drift section, approximately 1-m long in the LBL system, the electrons enter a further gap fed from a separate pulse line. Since the accelerator is driven by the rate of change of the magnetic field in the ferrite loop, the final electron energy achieved is equal to the energy acquired in a single gap multiplied by the number of gaps in use. In the LBL system each acceleration gap produced an electron energy gain of 0.25 MeV through the induction fields. The output energy of the electrons was 2.5 MeV, which was achieved with a repetition rate of about 5 pulses per second. In these experiments an electrostatic injector was used to provide a 1-MeV source for the electron beam. A new induction accelerator of this type is currently under construction at LLL.[116]

A variety of other devices that depend on the rate of change of flux through a circuit encircling the beam path have been described in the literature. These include the radial transmission pulse lines described by Pavlovskij et al.[117] and the Auto-accelerator described by Friedman and Lockner.[118] In both of these devices, which are shown in Figs. 16 and 17, the rate of change of flux is achieved through use of the distributed circuits illustrated, i.e., the

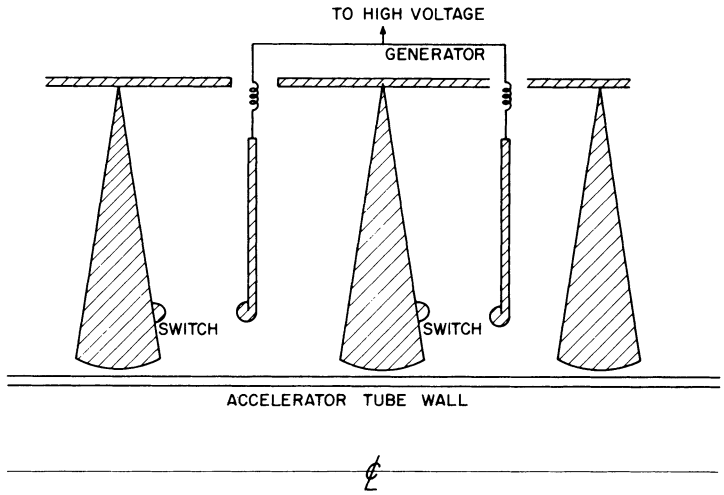

FIGURE 16 Section of an accelerator using radial transmission lines. The switches are closed, discharging the lines at times phased with the charged particle acceleration in the accelerator tube.

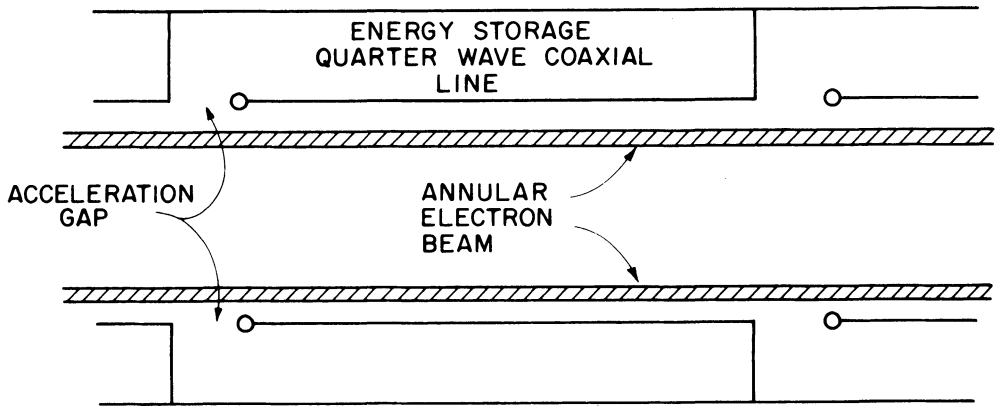

FIGURE 17 Section of an electron autoacceleration device.

change is produced by the propagation of an electromagnetic wave through an extended line, rather than through the lumped-parameter characteristics of the ferrite core of the LBL system. In Fig. 16 we show two sections of a radial-line induction accelerator. In this device, the electrons are accelerated by the fringing fields of the radial line. A series of appropriately sequenced switches short one side of each of the lines, so that the wave shorts out the voltage on the line in its initial transit. The wave is reflected from the open circut of the unloaded accelerating gap. Throughout the period that the wave propagates from the open circuit to the switch and is reflected back, the flux linked by the loop closed by the open circut gap on one side and the switch on the other, increases linearly in time. This rate of change of magnetic flux drives the electric field accelerating the charged particles across the gap. The acceleration achieved in each gap is cumulative as a result of the induction nature of the fields. Pavlovski projects that an accelerator of this type could be used to obtain electron beams with energies of order 10^5 J in the energy range of 10^6 to 10^7 eV.

The autoaccelerator system works on a different principle, but is of the same generic type as the induction accelerator. In this device, a slowly rising potential, applied to a vacuum diode, is used to produce a magnetically confined electron beam. After buildup of the beam to the required level, the beam is switched off rapidly by diverting the applied voltage from the gap through an auxilliary path. As a result of the beam propagation through the drift space, magnetic energy is stored in the concentric cavities. The beam current rapidly drops to about 20% of its peak level in about 5 nsec. Following the reduction in beam current the energy originally stored in the cavities cannot be maintained. The excess energy is transferred to the beam electrons as they cross the gaps and they are further accelerated. In this system, there is an automatic phase matching for the successive accelerating fields, since the cavity length equals the separation of the successive cavities and the electron velocity is essentially equal to the speed of light. This system, which has been successfully used with two cavities, is driven by the rate of change of flux in the cavities and hence belongs to the induction-linac family. Interstage cavity coupling appears to present some problems in the extension of this acceleration scheme to an arbitrarily large number of cavities.

An analysis of energy transfer in such devices has recently been reported by Eccelshall and Temperley.[119]

There has been a recent resurgence of interest in acceleration of moderate current beams to high energies, as a result of the heavy-ion fusion program. An approach to this problem being considered entails the use of linear induction accelerators for acceleration of high atomic number ($A \gtrsim 100$) materials to energies in the range of several GeV.[120] This approach and a separate program on intermediate atomic-number accelerators[121] have recently been initiated. In these systems, electrostatic acceleration will be used in the low-energy stages. Ions will be accelerated through a magnetically insulated diode, transported through an electrostatically neutralized section, and when all of the earlier-stage acceleration is complete, the tube in which the ions are buried will be pulsed so that the ions may be reaccelerated by a further magnetically insulated section. The final stages of the accelerator will use

induction acceleration. A variant of these schemes has been proposed by Winterberg.[122] Present induction accelerators have only been used for electron acceleration.

V. COLLECTIVE ACCELERATION

We conclude this report with a brief summary of progress and a report of current directions in collective acceleration. A number of previous reviews summarize this area,[123–129] so that only recent developments will be discussed. In collective ion accelerators, a high-power relativistic electron beam is used to accelerate a beam of positive ions to high energy. This process is achieved through the use of the collective fields of the primary electron beam. Work on this process was originated in the United States when Graybill and Uglam[130] first observed high-energy ions occurring when a high-current relativistic electron beam was injected into a low-pressure gas. Subsequent work has confirmed that it is relatively easy to achieve collective acceleration of the ions to energies corresponding to about three times the electron-beam energy, but that it has not been clear that this process can be scaled, for example, to achieve the high-energy (several hundred MeV) protons needed for electronuclear breeding. In addition to studies of collective acceleration of protons in electron beams, there has been additional work devoted to the acceleration of heavy ions. This work may have application to heavy-ion fusion sources and also to radio chemistry. Presently, achieved results indicate that collective accelerators may be competitive with cyclotrons for the generation of heavy ions in the 100 to 200 MeV range, and considerably cheaper. In the following section we shall present an account of the general results obtained and, in particular indicate directions presently being investigated for extension of this work to the high energies and fluxes required for projected applications.

Most of the research carried out to date has been centered on one of two areas, acceleration occurring when a high-current beam is injected into a low-pressure gas or into an evacuated tube through a dielectric anode. In the low-pressure gas case, the basis of the acceleration is at least qualitatively clear. A deep electrostatic potential well exists external to the anode and is separated from it by a distance of order c/ω_p.[131,132] The well is formed because the time taken to neutralize the beam space charge is long compared to the time taken for well formation and also because the current that can propagate in the unneutralized state is usually much smaller than the injected current. The well depth may, on a transient basis, exceed the diode accelerating potential and has been estimated to reach depths of between two and three times the diode potential difference. This potential well is in the sense that will accelerate ions from the vicinity of the anode parallel to the direction of the electron-beam propagation. The accelerated ions tend to neutralize the electron space charge and permit the beam to move from the diode region with a velocity approximately equal to the velocity acquired by the ions in falling through the potential well towards the virtual cathode. The correspondence between ion energy and the drift velocity of the beam has been verified experimentally.[133]

Generally most of the features observed in low-pressure gas acceleration are reasonably described by Olsen's detailed theory.[131] The observations which are reasonably accounted for include the cut-off in ion energy at about three times the beam energy, the short duration of the acceleration, the acceleration length scale and also the observed high-pressure cut off of the acceleration. At the higher pressures, one finds that the time scale to achieve a neutralized beam is comparable to or less than the acceleration time scale and hence acceleration ceases. Other models of the acceleration process have also been proposed, including the localized-pinch model.[134]

Consideration of energy balance[127,135] in propagating electron beams, coupled with an assumed beam-head acceleration, shows that conservation laws may impose serious limits on the achievable energies. This analysis also provides a description of the observed ion scaling with injection current and tube size. These scaling processes are not satisfactorily accounted for in the Olsen model. With the exception of ion acceleration occurring in high ν/γ beams, the observed acceleration has been limited to about three times the electron-beam energy. Of course, multiply charged ions have been detected and in these cases ion energies are scaled with the charge state. In the high ν/γ regime, the investment in reactive energy associated with beam transport is substantial, and the beam-head velocity is much less than the injection velocity of the electrons. Under such conditions, a high-energy contribution to the ion spectrum has been observed extending to about an order of magnitude greater energy than the beam electron energy.[136]

Much of the phenomenology described above is

equally applicable to the acceleration observed when a high-current electron beam is injected into an evacuated tube through a hole in a plastic anode. This configuration, which was first investigated by Luce et al.,[137,138] does, however, have a significant ion spectrum extending out to about twenty times the electron-beam energy. The phenomenon is once again related to the formation of virtual cathodes and deep potential wells. Ion acceleration has only been observed when the injected beam current exceeds the space-charge limit. Measurements with Rogowski coils also show that the propagating net beam current may exceed the space-charge limit and that magnetic neutralization occurs.[133] In fact, ion acceleration only appears to be important when magnetic neutralization of the beam is present. The high-energy tail is tacitly associated with the propagation of the well associated with the virtual cathode. Experiments have shown that in at least certain conditions the ion energy acquired is controlled by the velocity of the ions, i.e., deuterons have twice the energy of protons. The acceleration achieved appears to be limited by the available electron-beam momentum and will probably only be increased substantially by more efficient use of the electron momentum, either by reflexing of the electrons or by limiting the number of ions available, especially those at the low-energy end of the spectrum.[139] A variation on the Luce system[140,141] was recently investigated in which an attempt was made to control the beam propagation by injection into a dielectric-wall tube. In this configuration, proton acceleration up to about ten times the beam energy was achieved with a characteristic distribution function similar to that found in the Luce diode. In both the neutral-gas acceleration and the vacuum acceleration, the accelerating fields obtained exceed 1 MV/cm.

It should be noted that the dielectric-anode configuration has also been used for the acceleration of heavier ions. For example, the use of a teflon anode has resulted in the acceleration of fluorine ions to energies in excess of 135 MeV from a 2-MeV electron-beam generator.[137] Other experiments have been carried out in which the ions have been separately generated, using a laser beam or a puff valve, for provision of a localized ionized-gas region.[138] It may well be that the first useful application of collective accelerators is in the generation of medium-energy (a few hundred MeV) heavy ions.

Before discussing schemes presently being explored to attempt to control the ion acceleration, we point out a few of the observed limitations of the present schemes, and observations relevant to the theories of ion acceleration. For example, the deep potential well model implies the existence of wells with depths of up to three times the diode potential difference. Such wells should expel electrons. Efforts to search for high-energy electrons having energies up to three times the beam energy have failed,[139,142] the highest energy electrons being detected having only about 1.2 times the beam injection energy. Part of this may be accounted for by the fact that the wells are inherently transient in nature and can only exist dynamically. Electrons leaving the well will sample several oscillation periods of the well; hence we anticipate seeing only electrons with energies up to the average well depth. This appears to be the case in these experiments. One must therefore question the validity of the deep potential-well acceleration model, since the ion acceleration time is much greater than the well oscillation period.

Perhaps the most revealing information relating to the acceleration mechanism is the apparent failure to accelerate ions in the presence of a uniform magnetic guide field. Only two published observations have been reported in which acceleration occurred with magnetic guide fields.[143,144] In the first case the acceleration occurred when the electron beam was made to rotate by injection through a cusp field; the second occurred following the nonadiabatic expansion of the beam drift tube. In both cases, ion spectra extending to about or slightly greater than three times the beam energy were reported.

A number of experiments are currently in progress to control the ion acceleration. We shall describe briefly some of these efforts. Beam-head control is reported in two experiments (other experiments using pressure gradients to control beam-head velocity have been reported previously). The first of these uses a helix to surround the beam channel.[145] In this experiment, the pitch of the helix is changed so as to increase the velocity of the potential well at the beam head. The change in pitch of the helix has been selected to match the expected electric field causing the acceleration. It is too early to comment on the success of this experiment, but it is at least apparent that the beam-head acceleration is affected by the presence of the helix and that acceleration is only observed when the helix pitch is changed in the correct sense. The results obtained do not yet, however, yield any enhancement of the ion energy. The second experiment, which has not been in progress for a few years, provides active

control of the beam-head velocity. In this experiment a high-power laser is used, in conjuction with fiber optics, to externally spatially ionize a cesium channel at a predetermined rate. Accelerated ions will be generated from trace gases maintained in the acceleration chamber at densities too low to allow neutralization of the beam. Present progress has reached the point where control of the beam propagation has been demonstrated over a 10-cm channel. Acceleration rates corresponding to beam-head electric fields in the range of 0.1 to 1.0 MV/cm have been demonstrated.[146]

The second technique being investigated for the controlled collective acceleration of protons uses a negative-energy wave train grown on the electron beam propagating in vacuum. There are two experiments currently in progress to investigate the potential of variable phase-velocity wave trains to collective acceleration. The former, which has been extensively investigated theoretically,[147] uses a slow cyclotron wave on the electron beam. The wave is to be grown using either self-excitation in a helical structure surrounding the beam, or by imposing the desired wave frequency and wave number on the beam by propagation through a series of appropriately spaced resonant loop drives. In this experiment it is planned to accelerate protons to about 30 MeV using a 3-MeV electron beam.

The second system being used for acceleration in wave trains employs a slow space-charge wave grown on the beam during its propagation through a slow-wave structure.[143,149] In this experiment, wave growth, propagation, and coherence over a meter length of drift space has been demonstrated experimentally. Wave electric fields of about 50 kV/cm have been reported without evidence of saturation. In contrast to the cyclotron wave, the space-charge wave can only propagate at zero phase velocity at low frequency and at the space-charge limiting current. Present experiments indicate that useful velocities of as low as 0.2 c can be achieved and that this might go lower still with appropriate system design. In addition to investigating the variation of the phase velocity of the wave with the ratio of the current to limiting current, a preliminary experiment has been carried out to demonstrate the variation of the wave phase velocity in a drift tube. In this experiment, the demonstration of the principle entails accelerating protons from about 20 to 25 MeV in a meter or so of drift tube. Present experiments are devoted to injecting ions into a wave-growth region to establish the effect of the ion loading on the wave growth. It would seem that a linear-induction proton accelerator would be the most likely injection source for a practical accelerator.

It should be pointed out that the latter devices will, if they are successful, generate a reasonably monoenergetic ion beam with an energy spread limited to the well depth used for ion trapping. In scaling to multi-hundred MeV systems this would correspond to ion energy spectral widths of less than 0.25%.

Finally, we observe that other groups are now addressing wave acceleration experimentally[149,150,151] and that there are efforts under way to extend ion energies into the hundred megavolt range. These efforts include attempts to stage existing accelerator systems,[152] to proposed experiments where the high-energy ions can be produced through the adiabatic compression of proton rings.[153] As stated in the introduction, work on the electron-ring accelerator is proceeding but has not been discussed in this review. It should be noted, however, that recent results have demonstrated the acceleration of nitrogen ions to about 28 MeV.[154]

CONCLUSIONS

This review has been written with the object of outlining the current status of high-power electron and ion beam generation. By virtue of the breadth of the field the account is, of necessity, somewhat cursory.

We summarize the preceding sections by noting a few of the accomplishments in this rapidly developing area:

1. Electron and ion beam generators have been constructed and run at power levels of about one terawatt.
2. Diode and accelerator technology have advanced to the point where system behavior can be fairly confidently predicted.
3. Techniques have been established for the generation of ultrashort and also for moderate-length (few-microsecond) duration beams.
4. Devices have now been built with repetition rates as high as one hundred pulses per second.
5. A substantial number of applications of high-power beams have been identified and in some cases, e.g., high-power microwave generation, have been exploited to practical conclusions. Other applications include materials testing, x-ray generation, electron and ion beam fusion, and with the use of collective acceleration such diverse areas as

electro-nuclear breeding and radio-chemistry technology may become economically accessible.

6. Collective acceleration has reached a milestone in that people are now carrying out experiments to control the ion acceleration process instead of allowing nature to control the acceleration. Basic acceleration mechanisms are qualitatively understood, and equally importantly, heavy-ion collective acceleration is developing rapidly. It is presently at a stage where output ion energies competitive with those obtainable with cyclotrons have been produced.

ACKNOWLEDGEMENTS

I am grateful to my colleagues who have sent me reprints of their published work, and hence simplified the task of preparing this report. I am especially grateful to Richard Adler, David Hammer, Jim Ivers, Edward Ott, George Providakes, Victor Serlin, and Charles Wharton for their comments on the draft of this paper.

This work has been supported in part by AFOSR, BMDATC, and NSF.

REFERENCES

1. G. Yonas, J. W. Poukey, J. R. Freeman, K. R. Prestwich, A. J. Toepfer, M. J. Clauser, and E. H. Beckner, *Proceedings of Sixth European Conference on Controlled Fusion and Plasma Physics,* (Moscow, 1973), p. 483.
2. L. I. Rudakov, A. A. Samarsky, *Proceedings of Sixth European Conference on Controlled Fusion and Plasma Physics,* (Moscow, 1973), p. 487.
3. R. N. Sudan, *Proceedings of Sixth European Conference on Controlled Fusion and Plasma Physics,* (Moscow, 1973), p. 184.
4. L. S. Levine and I. M. Vitkovitsky, *IEEE Trans. Nucl. Sci.* **NS-18,** 255 (1971).
5. F. Winterberg, *Phys. Rev. 174,* 212 (1968).
6. H. H. Fleischmann, *Phys. Today* **28**(5), 35 (1975).
7. J. A.. Nation, *Appl. Phys. Lett.* **21,** 491 (1970).
8. M. Friedman and M. Herndon, *Phys. Rev. Lett.* **28,** 210 (1972).
9. S. E. Graybill and J. R. Uglum, *J. Appl. Phys.* **41,** 236 (1970).
10. J. Rander, B. Ecker, G. Yonas, and D. J. Drickey, *Phys. Rev. Lett.* **24,** 283 (1970).
11. V.I. Veksler, *Proceedings of CERN Symposium on High Energy Acceleration and Ion Physics,* (1956), Vol. I, p. 80.
12. T. H. Martin, *Proceedings of the International Pulsed Power Conference,* (Lubbock, Texas, 1976), ID1-1.
13. J. H. Nuckolls, *ERDA Summer Study of Heavy Ions for Inertial Fusion,* LBL-5543, p. 1, (1976).
14. N. C. Christofilos, *Proceedings of the 2nd United Nations International Conference on the Peaceful Uses of Atomic Energy,* **32,** 279 (1958).
15. L. S. Bogdankevitch, A. A. Rukhadze, *Soviet Phys. Uspekhi* **14,** 163 (1971).
16. J. A. Nation and M. E. Read, *Appl. Phys Lett.* **23,** 429 (1973).
17. M. E. Read and J. A. Nation, *J. Plasma Phys.* **13,** 127 (1975).
18. T. H. Martin, J. P. VanDevender, D. L. Johnson, D. H. McDaniel, and M. Aker, *Proceedings of the International Topical Conference on E-Beam Research and Technology,* (Albuquerque, New Mexico, 1975), p. 450.
19. B. Bernstein and I. Smith, *IEEE Trans. Nucl. Sci.* **NS-18,** 294 (1971).
20. R. A. Fitch and V. T. S. Howell, *Proceedings IEE,* (1964), Vol. III, p. 4.
21. T. H. Martin and R. S. Clark, *Rev. Sci. Instrum.* **47,** 460 (1976).
22. S. P. Bugaev, G. M. Kassirov, B. M. Kovalchuk, and G. A. Mesyats, *Zh. Eksp. Teor. Fiz. Pis'ma Red.* **18**(2), 92 (1973).
23. A. D. Blumlein, U.S. Patent No. 2,465,840 (March 29, 1948).
24. W. T. Link, *IEEE Trans. Nucl. Sci.* **NS-14,** 777 (1967).
25. S. E. Graybill and S. V. Nablo, *IEEE Trans. Nucl. Sci.* **NS-14,** 782 (1967).
26. K. R. Prestwich, *IEEE Trans. Nucl. Sci.* **NS-18,** 493 (1971).
27. T. H. Martin, *IEEE Trans. Nucl. Sci.* **NS-16**(3), 59 (1969).
28. F. M. Charbonnier, J. P. Barbour, J. L. Brewster, W. P. Dyke, and F. J. Grundhauser, *IEEE Trans. Nucl. Sci.* **NS-14,** 789 (1967).
29. J. D. Shipman, *IEEE Trans. Nucl. Sci.* **NS-18,** 294 (1971).
30. T. H. Martin, *IEEE Trans. Nucl. Sci.* **NS-22,** 289 (1975).
31. R. K. Parker, M. Ury, *IEEE Trans. Nucl. Sci.* **NS-22,** 983, (1975).
32. L. N. Kazansky, *Atomaya Energia* **42**(2), 113 (1977).
33. E. A. Abramyan, B. A. Altercop, and G. D. Kuleshov, *Proceedings of the Second International Topical Conference on High Power Electron and Ion Beam Research and Technology,* (Ithaca, New York, 1977), Vol. II, p. 743.
34. B. A. Demidov, M. V. Ivkin, V. A. Petrov, E. A. Smirnova, and S. P. Fanchenko, *Proceedings of the Second International Topical Conference on High Power Electron and Ion Beam Research and Technology,* (Ithaca, New York, 1977), Vol. II, p. 771.
35. J. C. Martin, *Internal Report SSWA/JCM/704/49,* AWRE, Aldermaston, England (1970).
36. J. P. VanDevender and T. H. Martin, *IEEE Trans. Nucl. Sci.* **NS-22,** 979 (1975).
37. *High Voltage Technology,* L. L. Alston, Ed., Oxford University Press (1968).
38. E. I. Baranchikov, A. V. Gordeev, V. D. Korolev, and V. P. Smirnov, *Proceedings of the Second International Topical Conference on High Power Electron and Ion Beam Research and Technology,* (Ithaca, New York, 1977), Vol. I, p. 3.
39. M. S. DiCapua, D. Pellinen, and P. D. Champney, *Proceedings of the Second International Topical Conference on High Power Electron and Ion Beam Research and Technology,* (Ithaca, New York, 1977), Vol. II, p. 781.

40. D. H. McDaniel, J. W. Poukey, K. D. Bergeron, J. P. VanDevender, and D. L. Johnson, *Proceedings of the Second International Topical Conference on High Power Electron and Ion Beam Research and Technology,* (Ithaca, New York,1977), Vol. II, p. 819.
41. A. A. Kolomensky, *Pis'ma JTP* **3,** 775 (1977).
42. R. K. Parker, R. E. Anderson, C. U. Duncan, *J. Appl. Phys.* **45,** 2463 (1976).
43. J. J. Clark, M. Ury, M. L. Andrews, D. A. Hammer, and S. Linke, *Record of the 10th Symposium on Electron, Ion, and Laser Beam Technology,* San Francisco Press, (1969), p. 117.
44. P. A. Miller, J. W. Poukey, and T. P. Wright, *Phys. Rev. Lett.* **35,** 940 (1975).
45. P. Diament, *Phys. Rev. Lett.* **37,** 168 (1976).
46. M. Reiser, *Phys. Fluids* **20,** 477 (1977).
47. M. Friedman and M. Ury, *Rev. Sci. Instrum.* **41,** 1334 (1970).
48. F. Friedlander, R. Hechtel, H. Jory, and C. Mosher, *Varian Associates Report* DASA-2173 (1968), unpublished.
49. G. Yonas, J. W. Poukey, K. R. Prestwich, J. R. Freeman, A. J. Toepfer, and M. J. Clauser, *Nucl. Fusion* **14,** 731 (1974).
50. D. dePackh, *NRL Radiation Progress Report* 5 (1968), unpublished; D. dePackh, *NRL Radiation Progress Report* 17 (1969), unpublished.
51. J. M. Creedon, *J. Appl. Phys.* **46,** 2946 (1975).
52. S. A. Goldstein, R. C. Davidson, J. G. Siambis, and R. Lee, *Phys. Rev. Lett.* **33,** 1471 (1974).
53. J. Poukey, J. W. Freeman, and G. Yonas, *J. Vac. Sci. Technol.* **10,** 954 (1973).
54. J. Poukey and A. J. Toepfer, *Phys. Fluids* **17,** 1582 (1974).
55. D. L. Morrow, J. D. Phillips, R. M. Stringfield, W. O. Doggett, W. H. Bennett, *Appl. Phys. Lett.* **19,** 444 (1971).
56. W. C. Condit, D. O. Trimble, G. A. Metzger, D. G. Pellinen, S. Heurlin, and P. Creely, *Phys. Rev. Lett.* **30,** 123 (1973).
57. L. P. Bradley, G. W. Kuswa, *Phys. Rev. Lett.* **29,** 1441 (1972).
58. M. DiCapua, J. Creedon, and R. Huff, *J. Appl. Phys.* **47,** 1887 (1976).
59. A. Blaugrund, G. Cooperstein, and S. Goldstein, *Phys. Fluids* **20,** 1185 (1977).
60. G. Cooperstein and J. J. Condon, *J. Appl. Phys.* **46,** 1535 (1975).
61. A. E. Blaugrund and G. Cooperstein, *Phys. Rev. Lett.* **34,** 461 (1975).
62. J. W. Poukey, *Appl. Phys. Lett.* **26,** 145 (1975).
63. J. W. Poukey, *J. Vac. Sci. Technol.* **12,** 1214 (1975).
64. S. A. Goldstein and R. Lee, *Phys. Rev. Lett.* **35, 1079** (1975).
65. A. E. Blaugrund, G. Cooperstein, and S. Goldstein, *Proceedings of the International Conference on Electron Beam Research and Technology,* (Albuquerque, New Mexico, 1975), p. 223.
66. J. Poukey, *Appl. Phys. Lett.* **26,** 145 (1975).
67. S. Humphries, J. J. Lee, and R. N. Sudan, *Appl. Phys. Lett.* **25,** 20 (1976).
68. S. Humphries, J. J. Lee, and R. N. Sudan, *J. Appl. Phys.* **46,** 187 (1975).
69. S. Humphries, R. N. Sudan, and W. Condit, *Appl. Phys. Lett.* **26,** 667 (1975).
70. J. Golden, C. A. Kapetanakos, S. J. Marsh, and S. Stephanakis, *Phys. Rev. Lett.* **38,** 130 (1977).
71. C. A. Kapetankos, J. Golden, W. M. Black, *Phys. Rev. Lett.* **37,** 1236 (1977).
72. D. S. Prono, J. W. Shearer, and R. J. Briggs, *Phys. Rev. Lett.* **37,** 21 (1976).
73. D. S. Prono, J. M. Creedon, I. Smith, and N. Bergstrom, *J. Appl. Phys.* **46,** 3310 (1975).
74. H. H. Fleischmann, *Proceedings of Conference on Electrostatic and Electromagnetic Confinement of Plasmas and Phenomenology of Relativistic Electron Beams,* (N.Y. Academy of Science, 1974), p. 472.
75. H. H. Fleischmann and T. Kammash, *Nucl. Fusion* **15,** 1143 (1975).
76. C. A. Kapetanakos and R. Parker, *Appl. Phys. Lett.* **26,** 284 (1975).
77. T. Antonsen and E. Ott, *Phys Fluids* **19,** 52 (1976).
78. T. Antonsen and E. Ott, *Appl. Phys. Lett.* **28,** 424 (1976).
79. J. M. Creedon, I. D. Smith, and D. S. Prono, *Phys. Rev. Lett.* **35,** 91 (1975).
80. J. Golden, C. A. Kapetanakos, R. Lee, and S. Goldstein, *Proceedings of the International Topical Conference on Electron Beam Research and Technology,* (Albuquerque, New Mexico, 1975), p. 635.
81. J. A. Pasour, R. A. Mahaffey, J. Golden, and C. A. Kapetanakos, *Phys. Rev. Lett.* **40,** 448 (1978).
82. P. Drieke, C. Eichenberger, S. Humphries, and R. N. Sudan, *J. Appl. Phys,* **47,** 85 (1976).
83. S. Humphries, R. N. Sudan, and L. Wiley, *J. Appl. Phys.* **47,** 2382 (1976).
84. T. J. Orzechowski and G. Bekefi, *Phys. Fluids* **19,** 43 (1976).
85. S. C. Luckhardt and H. H. Fleischmann, *Appl. Phys. Lett.* **30,** 192 (1977).
86. S. Luckhardt, H. H. Fleischmann, and R. Kribel, to be pulished, see also, *Bull. Am. Phys. Soc.* **23**(7), 816 (1978).
87. R. N. Sudan and R. V. Lovelace, *Phys. Rev. Lett.* **31,** 1174 (1973).
88. R. V. Lovelace and E. Ott, *Phys. Fluids* **17,** 1263 (1974).
89. A. Ron, A. A. Mondelli, and N. Rostoker, *IEEE Trans. Plasma Sci.* **PS-1,** 85 (1973).
90. K. Bergeron and J. Poukey, *Appl. Phys. Lett.* **27,** 58 (1975).
91. K. Bergeron, *Phys. Fluids* **20,** 688 (1977).
92. G. Kuswa, S. Humphries, D. Johnson, R. Leeper, and J. Freeman, *Proceedings of the Second International Topical Conference on High Power Electron and Ion Beam Research and Technology,* (Ithaca, New York, 1977), Vol. I, p. 99.
93. M. Greenspan, S. Humphries, J. Maenchen, and R. N. Sudan, *Phys. Rev. Lett.* **39,** 24 (1977).
94. J. Creedon, *J. Appl. Phys.* **48,** 1070 (1977).
95. K. Bergeron, *J. Appl. Phys.* **48,** 3065 (1977).
96. J. Poukey and K. Bergeron, *Appl. Phys. Lett.* **32,** 8 (1978).
97. I. Smith, P. Champney, and J. Creedon, *Proceedings of the International IEEE Pulsed Power Conference,* (New York, 1976), Vol. II, C-8.
98. M. DiCapua, D. Pellinen, P. Champney, and D. McDaniel, *Proceedings of the Second International Topical Conference on High Power Electron and Ion Beam Research and Technology,* (Ithaca, New York, 1977), Vol. II, p. 781.
99. D. McDaniel, J. Poukey, K. Bergeron, J. VanDevender,

and D. Johnson, *Proceedings of the Second International Topical Conference on High Power Electron and Ion Beam Research and Technology,* (Ithaca, New York, 1977), Vol. II, p. 819.
100. J. Poukey, J. Freeman, M. Clauser, and G. Yonas, *Phys. Rev. Lett.* **35,** 1806 (1975).
101. J. Poukey, *J. Vac. Sci. Technol.* **12,** 1214 (1975).
102. S. Stephanakis, D. Mosher, G. Cooperstein, J. Boller, J. Golden, and S. Goldstein, *Phys. Rev. Lett.* **37,** 1543 (1976).
103. P. Gilad and Z. Zinamon, *Phys. Rev. Lett.* **37,** 697 (1976).
104. P. Gilad, S. Miller, and Z. Zinamon, *Appl. Phys. Lett.* **31,** 151 (1977).
105. S. Miller and Z. Zinamon, *Phys. Rev. Lett.* **36,** 1303 (1976).
106. D. Mosher, G. Cooperstein, S. J. Stephanakis, S. Goldstein, D. Colombant, and R. Lee, *Proceedings of the Second International Topical Conference on High Power Electron and Ion Beam Research and Technology,* (Ithaca, New York, 1977), Vol. I, p. 257.
107. P. Gilad, Z. Kaplan, S. Miller, J. Wachtel, N. Zeiberg, and Z. Zinamon, *Proceedings of the Second International Topical Conference on High Power Electron and Ion Beam Research and Technology,* (Ithaca, New York, 1977), Vol. I, p. 219.
108. D. Swain, S. Goldstein, L. Mix, J. Kelley, G. Hadley, *J. Appl. Phys.* **48,** 1085 (1977).
109. R. Adler and J. Nation, unpublished.
110. M. Read and J. Nation, *J. Appl. Phys* **47,** 5236 (1976).
111. G. Yonas, K. Prestwich, J. Poukey, and J. Freeman, *Phys. Rev. Lett.* **30,** 164 (1973).
112. G. J. Rohwein, M. Buttram, and T. Prestwich, *Proceedings of the Second International Topical Conference on High Power Electron and Ion Beam Research and Technology,* (Ithaca, New York, 1977), Vol. II, p. 845.
113. R. Faltens and D. Keefe, (1970), unpublished; R. T. Avery et al., *Proceedings of the IEEE Accelerator Conference,* (1971), **NS-18,** p. 479.
114. J. Beal, N. Christofilos, and R. Hester, *Proceedings of the IEEE Accelerator Conference,* (1969), p. 294.
115. J. F. Leiss, *Proceedings of the Proton Linac Conference,* (1972), p. 197.
116. R. Hester, L. Reginato, A. Chesterman, and A. Faltens, to be presented at the IEEE Accelerator Conference, (San Francisco, 1979).
117. A. I. Pavlovskij, V. S. Bosamykin, G. Kuleshov, A. Gerasimov, V. Tenanakin, and A. Klement'ev, *Dokl. Akad. Nauk SSSR* **222,** 817 (1975).
118. T. Lockner, J. Siambis, and M. Friedman, *Proceedings of the Second International Topical Conference on High Power Electron and Ion Beam Research and Technology,* (Ithaca, New York, 1977), Vol. II, p. 585.
119. D. Eccleshall and J. Temperley, *J. Appl. Phys.* **49,** 3669 (1978).
120. A. Faltens and D. Keefe, *LBL Report* 6453 (1977).
121. S. Humphries, *J. Appl. Phys.* **49,** 501 (1978).
122. F. Winterberg, *Z. Physik A.* **280,** 359 (1977).
123. G. Yonas, *Particle Accelerators* **5,** 81 (1973).
124. M. Rabinovich and V. N. Tsytovich, *Particle Accelerators* **5,** 99 (1973).
125. A. Kolomensky, *Particle Accelerators* **5,** 73 (1973).
126. C. Olsen, *Particle Accelerators* **6,** 107 (1974).
127. S. Putnam, Presented at 2nd Symposium on Collective Methods of Acceleration, (Dubna, USSR, 1976), *Physics International Report* PIIR-7-76.
128. Ya. B. Fainberg, *Particle Accelerators* **6,** 95 (1976).
129. C. Olsen, *Sov. J. Plasma Phys.* **3**(3), 259 (1978).
130. S. Graybill and J. Uglam, *J. Appl. Phys.* **41,** 236 (1970).
131. C. Olsen, *Phys. Fluids* **18,** 585 (1975); C. Olsen, *Phys. Fluids* **18,** 598 (1975).
132. J. Poukey and N. Rostoker, *Plasma Phys.* **13,** 897 (1971).
133. R. Miller and D. Straw, *J. Appl. Phys.* **47,** 1897 (1976).
134. S. Putnam, *Phys. Rev. Lett.* **25,** 1129 (1970).
135. V. N. Tsytovich and K. V. Khodataev, *Comments on Plasma Physics and Controlled Fusion* **3,** 71 (1977).
136. B. Ecker and S. Putnam, *IEEE Trans. Nucl. Sci.* **NS-24,** 1665 (1977).
137. J. S. Luce, *Annals of the N.Y. Acad. of Sci.* **25,** 2171 (1975).
138. W. Destler and H. Kim, *Proceedings of the Second International Topical Conference on High Power Electron and Ion Beam Research and Technology,* (Ithaca, New York, 1977), Vol. II, p. 521.
139. R. Adler and J. Nation, *Cornell University Laboratory of Plasma Studies Report* 225 (1978), to be published.
140. A. Greenwald and R. Little, *Proceedings of the Second International Topical Conference on High Power Electron and Ion Beam Research and Technology,* (Ithaca, New York, 1977), Vol. II, p. 553.
141. J. A. Pasour, R. Parker, W. Doggett, D. Pershing, and R. Gullickson, *Proceedings of the Second International Topical Conference on High Power Electron and Ion Beam Reseach and Technology,* (Ithaca, New York, 1977), Vol. II, p. 623.
142. R. Adler, G. Gammel, J. Nation, G. Providakes, and R. Williams, *Proceedings of the Third International Conference on Collective Methods of Acceleration,* (Laguna, Beach, 1978), to be published. Also, *Cornell University LPS Report* 248 (1978).
143. C. W. Roberson, S. Eckhouse, A. Fisher, S. Robertson, and N. Rostoker, *Phys. Rev. Lett.* **36,** 1457 (1976).
144. S. Eckhouse, A. Fisher, R. Mako, C. W. Roberson, S. Robertson, and N. Rostoker, *Proceedings of the Second International Conference on Collective Methods of Acceleration,* (Dubna, 1976), p. 9i.
145. W. Destler, H. Kim, G. Zorn, and R. Hoeberling, presented at Third International Conference on Collective Methods of Acceleration, (Laguna Beach, 1978), to be published.
146. C. Olsen, presented at Third International Conference on Collective Methods of Acceleration, (Laguna Beach, 1978), to be published.
147. M. Sloan and W. Drummond, *Phys. Rev. Lett.* **31,** 1234 (1973).
148. R. Adler, G. Gammel, J. A. Nation, M. E. Read, R. Williams, P. Sprangle, and A. Drobot, in *Proceedings of the Second International Topical Conference on High Power Electron and Ion Beam Research and Technology,* (Ithaca, New York, 1977), Vol. II, p. 509.
149. P. Sprangle, A. Drobot, and W. Manheimer, *Phys. Rev. Lett.* **36,** 1180 (1976).
150. S. Yadavelli, *Appl. Phys. Lett.* **29,** 272 (1976).
151. P. Sprangle, private communication.
152. J. Adamski, P. Wei, J. Beymer, R. Guay, and R. Copeland, in *Proceedings of the Second International Topical Conference on High Power Electron and Ion Beam Research and Technology,* (Ithaca, New York, 1977), Vol. II, p. 497.
153. H. H. Fleischmann, *Proceedings of Conference on Elec-*

trostatic and Electromagnetic Confinement of Plasma's and Phenomenology of Relativistic Electron Beams, (N.Y. Acad. Sci., 1974), p. 472.

154. V. P. Sarantsev, *Proceedings of the Third International Conference on Collective Methods of Acceleration,* (Laguna Beach, 1978), to be published.